DEVELOPMENT OF ALTERNATIVE PHARMACEUTICAL ANALYSIS BY
SMARTPHONE-BASED COLORIMETRY

By

MISS Noppharat PHADUNGCHAROEN

A Thesis Submitted in Partial Fulfillment of the Requirements
for Doctor of Philosophy (PHARMACEUTICAL SCIENCES)
Graduate School, Silpakorn University
Academic Year 2021
Copyright of Silpakorn University

การพัฒนาเภสัชวิเคราะห์ทางเลือกโดยการวัดสีด้วยสมาร์ตโฟน

โดย
นางสาวนพรัตน ผดุงเจริญ

วิทยานิพนธ์นี้เป็นส่วนหนึ่งของการศึกษาตามหลักสูตรปรัชญาดุษฎีบัณฑิต
สาขาวิชาวิทยาการทางเภสัชศาสตร์ แบบ 1.2 ปรัชญาดุษฎีบัณฑิต
บัณฑิตวิทยาลัย มหาวิทยาลัยศิลปากร
ปีการศึกษา 2564

DEVELOPMENT OF ALTERNATIVE PHARMACEUTICAL ANALYSIS BY SMARTPHONE-BASED COLORIMETRY

By

MISS Noppharat PHADUNGCHAROEN

A Thesis Submitted in Partial Fulfillment of the Requirements
for Doctor of Philosophy (PHARMACEUTICAL SCIENCES)
Graduate School, Silpakorn University
Academic Year 2021
Copyright of Silpakorn University

Title	Development of alternative pharmaceutical analysis by smartphone-based colorimetry
By	MISS Noppharat PHADUNGCHAROEN
Field of Study	(PHARMACEUTICAL SCIENCES)
Advisor	Associate Professor Theerasak Rojanarata, Ph.D.
Co advisor	Professor PRANEET OPANASOPIT, Ph.D.

Graduate School Silpakorn University in Partial Fulfillment of the Requirements for the Doctor of Philosophy

.... Dean of graduate school
(Associate Professor Jurairat Nunthanid, Ph.D.)

Approved by

.... Chair person
(Assistant Professor MALAI SATIRAPHAN, Ph.D.)

.... Advisor
(Associate Professor Theerasak Rojanarata, Ph.D.)

.... Co advisor
(Professor PRANEET OPANASOPIT, Ph.D.)

.... External Examiner
(Assistant Professor Samarwadee Plianwong, Ph.D.)
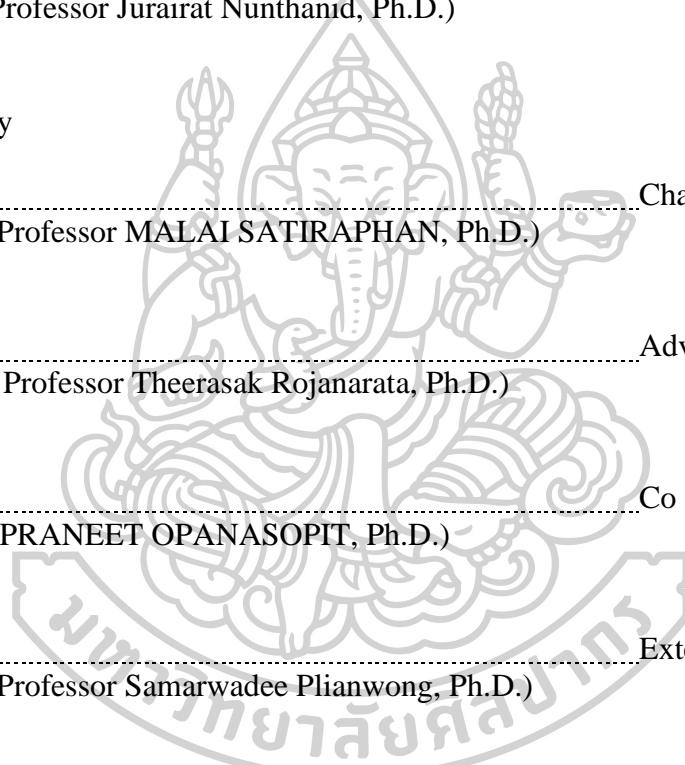
MISS NOPPHARAT PHADUNGCHAROEN : DEVELOPMENT OF ALTERNATIVE PHARMACEUTICAL ANALYSIS BY SMARTPHONE-BASED COLORIMETRY THESIS ADVISOR : ASSOCIATE PROFESSOR THEERASAK ROJANARATA, Ph.D.

While smartphone-based colorimetry has gained popularity for the analysis of various substances, its application to drug analysis is currently limited. Therefore, the aim of this work was to develop facile, rapid and cost-effective alternative pharmaceutical assays relying on smartphone-based methods. In overall, the drugs were analyzed under the optimized condition and the images were captured using smartphone. The colors of image were then interpreted to RGB pixels and the values were used as the analytical signal to establish the linear relationship to drug concentration. To confirm the reliability of the assays, the methods were validated and the results were compared with that obtained from standard methods. In the first work, colorimetric method was developed for the quantitation of a thiol-containing drug namely D-penicillamine based on the formation of yellow color after the reaction using Ellman's reagent. Log B_0/B, when B_0 was B value of a blank, showed a good relationship to drug concentration, with an R^2 of 0.9996. The LOD and LOQ of 0.44 µg/mL and 1.32 µg/mL, respectively, were adequate for the assay of penicillamine capsules. Besides, the method was capable of quantitating thiol groups in thiolated chitosan, giving comparable analytical results to that obtained from the absorbance measurement. In the second work, the assay of chlorpromazine hydrochloride was developed based on the formation of ion-pair complex of the drug and methyl orange in microcentrifuge tubes, followed by the extraction of the complex into ethyl acetate, resulting in yellow colored organic phase. The image was captured while the two phases were in the tube. $B/(R+G+B)$ gave the best relationship to drug concentration, with an R^2 of 0.9998. The method was fast and safe due to a lack of the transfer of organic phase out of the tubes for the measurement. Moreover, by aligning as many as 24 tubes in a radial pattern, multi-samples could be simultaneously and rapidly analyzed without the variation effects from the position of tubes during the photography. In the last work, smartphone-based colorimetry was applied to determine the equivalence point of a miniaturized Volhard's titration of sodium chloride injection. The method was conducted by plotting a linear segment curve of $1/\log G$ which correlated to the reddish orange color intensity and the volumes of titrant. The equivalence point was then determined by the intersection of the two straight lines located in the regions before and after the equivalence point. The method showed a good linear correlation of the titrant volume at the equivalence point and sodium chloride concentration in the range of 0.42% to 0.97% w/v with an R^2 of 0.9998, indicating its applicability for quality control of 0.45% and 0.90% w/v sodium chloride injections. As proven by validation results, all the methods developed in this work were accurate, precise, and specific. There were no significant differences between these methods and the USP methods. Therefore, smartphone-based colorimetry was a good alternative for pharmaceutical analysis.

ACKNOWLEDGEMENTS

TABLE OF CONTENTS

Page

LIST OF TABLES

LIST OF FIGURES

Page

LIST OF ABBREVIATIONS

%	percentage
/	divide
®	registered trademark
>	more than
≥	more than or equal
<	less than
°C	celsius degree
et al.	et alia (Latin) means "and others"
i.e.	id est (Latin) means "That is"
e.g.	exempli gratia (Latin) means "for example"
etc.	et cetera (Latin) mean "and other similar things"
h	hour(s)
min	minute(s)
s	second(s)
L	liter
mL	milliliter
μL	microliter
g	gram
mg	milligram
μg	microgram
M	molar

mM	millimolar
µM	micromolar
N	normality
w/v	weight by volume
v/v	volume by volume
cm	centimeter
nm	nanometer
ANOVA	analysis of variance
ALS	ambient Light Sensor
$AgNO_3$	silver nitrate
CPZ	chlorpromazine
CMOS	complementary Metal Oxide Semiconductor
CCDs	charge-Coupled Devices
CF	color Filter
CIE	the commission International de l'Eclairage
DNA	deoxyribonucleic Acid
DLLME	dispersive liquid-liquid microextraction
EDTA	ethylenediaminetetraacetic acid
GPS	global positioning system
HPLC	high performance liquid chromatography
ICH	the international council for harmonization
Log	logarithm
LOD	limit of detection

LOQ	limit of quantification
LED	light emitting diode
LA	labeled amounts
MO	methyl orange
NaCl	sodium chloride
NH_4SCN	ammonium thiocyanate
NSS	normal saline solution
NSAIDs	non-steroidal anti-inflammatory drugs
pH	potentia hydrogenii (latin)
Q	the quantity
R.S.D.	relative standard deviation
S.D.	standard deviation
TNB	2-nitro-5-thiobenzoic acid
UV	ultraviolet
USP	the united state pharmacopeia
Vis	visible
3D	3 dimensions

CHAPTER 1
INTRODUCTION

1.1 STATEMENT AND SIGNIFICANCE OF THE RESEARCH PROBLEM

Nowadays, smartphone plays an important role in a daily life. Various functions are used to support the living through its intelligent sensor and operating system. Considering the portability, functional ease, and cost of smartphones compared to laboratory equipment, smartphone can be adapted in the analytical technique in term of color reading by using the built-in camera for the colorimetric assay. Traditionally, colorimetry is performed in combination with a naked eye examination, or more precisely, using spectroscopic instruments such as spectrophotometers in which the color intensity is measured through the absorption of light as a function of wavelength and solute concentration according to the Beer–Lambert's law. Practically, there are series of repeating steps involved in the analysis of a set of samples, for example, the transfer of a solution into a cuvette, the measurement, cuvette rinsing, cleaning, and repetition of the process for the new measurement. The procedure is time consuming and enhances risks of contamination and chemical contact. Although the spectral measurement provides effective means to quantify colors, the devices are generally expensive, bulky, and confined to operate under laboratory settings. Hence, the use of handheld or portable devices with cost-effective optoelectronic components has recently become an attractive alternative. Smartphones showed the efficiency to quantify various substances based on direct colorimetric reaction. However, there were a few reports that studied the use of smartphone-based colorimetry for pharmaceutical analysis [1, 2] though colorimetry has been commonly used in the pharmaceutical analytical process, especially, the assay. Therefore, the use of smartphone-based colorimetry in the pharmaceutical assay has become an interesting method. Among pharmaceutically important thiol-containing compounds, penicillamine, captopril, enalapril, and 6-mercaptopurine required high-performance liquid chromatography (HPLC) for their assay according to the standard method reported in the international pharmacopeia i.e., USP. Thus, the method is rather complex and needed an expensive instrument. On the other hand, a

simpler method to quantify the free thiol containing compounds has been discussed which is the colorimetric reaction of Ellman's reagent. This reagent directly reacts with the thiol group resulting the release of a yellow compound which can be measured spectrophotometrically. The Ellman's method was used for the determination of pharmaceutical compound, i.e. captopril tablet assay [3] and penicillamine assay in biological fluid [4]. D-penicillamine is a thiol containing molecule which is an important drug for inflammatory disease and plays a role to bind copper ion and remove it from body in Wilson's disease. Several approaches have been used for penicillamine determination such as UV–visible spectrophotometry [5-7], fluorospectrometry [8, 9], HPLC [10], flow injection analysis [11], capillary electrophoresis [12], etc. However, Ellman's reaction has rarely been reported to be applied with a smartphone for colorimetry, especially for the determination of D-penicillamine, which has not been reported. Therefore, it was investigated in this work. Moreover, this study would extend the use of smartphone-based colorimetry with Ellman's reaction for the assay of thiol-containing polymers.

In the analytical process, the liquid-liquid extraction is a conventional method used for the separation of compounds which have different solubility. The major drawback of extraction is the use of large volume of toxic organic solvent increasing the health risk to analyst. So, a small-scale extraction and using low toxic solvent become the points of interest. After the extracted compound is obtained, it will be analyzed by different technique. Herein, colorimetry could be used in the analysis for the quantitation of extracted compounds. Chlorpromazine hydrochloride (CPZ) is an important drug in the group of phenothiazine and is used for psychoses control which was reported by using various assay methods such as HPLC [13], nuclear magnetic resonance spectroscopy (NMR) [14], including liquid-liquid extraction [10]. However, it has not been reported to be quantitated by smartphone-based assay. To develop more safe method for CPZ extraction, the scale reduction would be studied. A mini-scale ion pair extractive assay for chlorpheniramine maleate was published, with the amount of organic extractant utilized limited to 500 μL per sample [15]. Nonetheless, the process was designed for the organic phase to be transferred. Furthermore, measuring the absorbance of a few microliters of the aqueous phase

following back-extraction necessitates the use of a drop-based spectrophotometer, which is not a common equipment in chemical laboratory. Because of the benefits of smartphone, which is low cost and easy to use over laboratory equipment, therefore, the smartphone-based colorimetry was developed relying on small scale ion-pair extraction for the assay of CPZ.

Titration is another method used in the analysis of drug content. In the common titration, an end point observation and the interpretation of result are done by the analyst in which the human error can occur due to its low accuracy to detect color change and to read the titrant volume used. To improve the precision, smartphone could be adapted. Smartphone was reported to be used for the end point detection of acid-base titration which was performed in a volumetric flask in a normal titration scale. The end point was investigated from the detection of color change by application on smartphone and the RGB measurement [16, 17]. Although these reports was successful to reduce the human error of end point detection, the error of the titrant volume reading still exist. Normally, the equivalence point can be determined by finding an inflection point (the point of maximum slope or sharp break) of the curve or by calculating the maximum of the first derivative plot or the zero of the second derivative plot. Alternatively, plotting two straight lines from the data of a certain solution's property measured on both sides of the equivalence point results in another type of titration curve called a linear-segment curve. Therefore, a smartphone-based colorimetry was developed to work together with linear segment curve to minimize the error from end point detection and titrant volume reading.

The miniaturized Volhard's titration is a small-scale titration used for the assay of chloride ion. It was reported for the sodium chloride assay by titrating in 1.5-mL microcentrifuge tube [18, 19]. However, the method was required an expensive UV-vis spectrophotometer to measure the absorbance. To develop more convenient and low-cost detector, the smartphone is an attractive alternative. Hence, in this work, smartphone-based colorimetry was applied to a small-scale Volhard's titration by using sodium chloride injection, which is a pharmaceutical product, to be a model drug.

As aforementioned, smartphone-based colorimetric methods enabled the improvement of colorimetry in which the method would be saver in term of the amount of solvent, cost, and time of the analysis and be safe for human. In this thesis, smartphone was applied to perform the green colorimetry for the assay of pharmaceutical substances and improve the assay method of the pharmaceutical products based on three analytical methods which were colorimetry rely on Ellman' s assay, ion-pair extraction, and Volhard's titration.

1.2 OBJECTIVES

1.2.1. To develop a smartphone-based Ellman's assay.

1.2.2. To develop a smartphone-based ion-pair extraction.

1.2.3. To develop a smartphone-based titration relying on Volhard's method.

1.3 HYPOTHESES

1.3.1. The proposed methods can be used for pharmaceutical assay, i.e., D-penicillamine, cysteine conjugated chitosan, chlorpromazine hydrochloride, and sodium chloride.

1.3.2. The proposed methods were simple, fast, cost-effective, and safe.
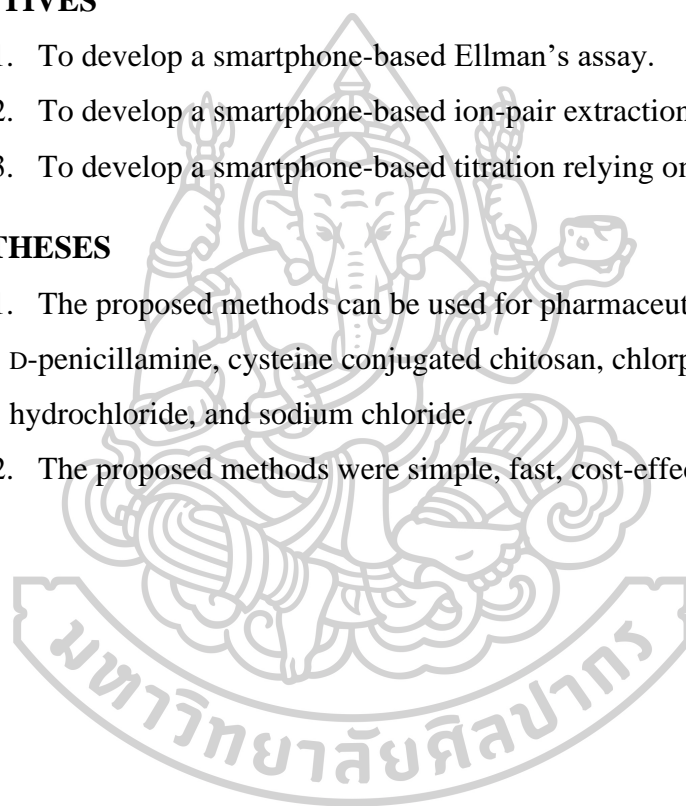
CHAPTER 2
LITERATURE REVIEW

2.1 SMARTPHONE

In the present day, smartphones have evolved into a worldwide technology with superior features and sensors. It has been used for more than simply communication; it has also been used to make life easier. Figure 1 shows common smartphone sensors in the recent. The accelerometer and gyroscope in smartphones are motion sensors that detect the smartphone's direction and movement in three dimensions and rotation, respectively. Another one of well-known sensor and be worked with other motion sensor for the best navigator is the Global Positioning System (GPS) sensor. Radio waves was used to communicate between smartphone and satellites, then providing location data back in which the most of the world's locations can be displayed in a fraction of a second on smartphone [20]. This device also includes a variety of sensors, such as an ambient light sensor (ALS), humidity sensor, microphone and camera sensor.
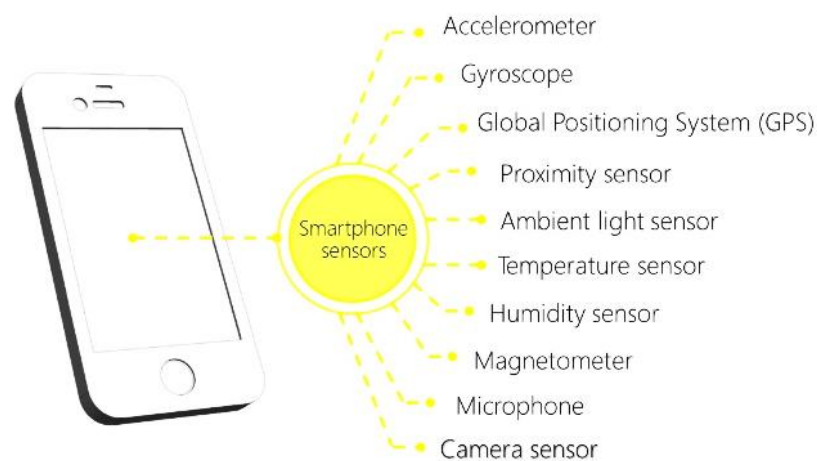
Figure 1. Sensors in smartphones.

2.1.1 Smartphone camera

For a long time, the smartphone camera has been used as a marketing tool. It was created to provide a higher quality image by increasing the size and resolution of

the image sensor. An image sensor is a piece of electrical equipment that turns an optical picture into an electronic signal. There are two main types of image sensor used in the resent including a complementary metal oxide semiconductor (CMOS) image sensor and a charge-coupled devices (CCD) image sensor.

A CMOS image sensor is the most common type of sensor found in smartphones. It operates simply by converting a light signal to an electric charge at a pixel site of image sensors, allowing for quick and flexible processing. When opposed to CMOS, the CCD image sensor will transform photon signals into analog data on a pixel site and transmit it to another convertor to convert the analog signal to a digital signal, resulting in a higher quality image. However, it is only employed in a few phone cameras because to the following drawbacks: sophisticated work processing, many steps required for signal conversion, higher space on a chip, higher power consumption, and expensive cost [21].

2.2 SMARTPHONE IN RESEARCH WORK

New technology was developed every year including smartphone. High capacity and multifunctional of smartphone have been useful for many purposes, not only for communication. For education, Bandyopadhyay S. adapted smartphone as an assistive tool to detect titration endpoint for color-blind [17]. The developed application on smartphone work with camera sensor and audio sensor to detect color of titration and alert by giving vibration and sound feedback to aid impaired student for learning. Additionally, smartphones were used in Physics class to help students learn educational elements quickly and process experimental data at any time and from any location, as well as to support collaboration between teacher and student by designing real experiments with low-cost equipment [22].

Because it was necessary and carried with the owner almost all of the time, the smartphone was used to track social behavior. Mood tracking application and GPS sensor work together to record the relationship between personality and feeling of that person when be in any location which has psychologically meaningful [23, 24]. Moreover, smartphone usage data can show the relation of the depressive symptom severity of user, improving clinical opportunities and continuous monitoring of patient [25]. Apart from social behavior study, advanced smartphone technology

showed a role in healthcare system to be a monitoring and diagnosis tools of many organs including heart [26], lung [27], ophthalmic system [28], skin [29] and hearing system [30, 31]. The smartphone and its embedded sensors open up a new opportunity to improve healthcare services by allowing data to be transferred quickly and easily over the internet for further investigation [32].

Smartphone was studied for a long time in pure sciences. Smartphone-based method is useful for limited areas and budgets because to their low cost, portability, and low power requirements. Since the analysis of trace element to large molecule or chemical and biological substances, smartphone can analyze an expressed color of reaction in visible range, which relate to amount or concentration of interested substance, by using its camera. In environmental studies or pollutant control, on-site sample quantitation is a high-potential activity. Hence, a small device that can work all-in-one is the best requirement for the most convenient technique. Not only for water testing, soil nutrient and air pollutant were also studied. An important ion and trace element in water, soil, and food, for example ammonia [33], chlorine [34], calcium [35], curcumin in turmeric [36], heavy metal [37-39] and include dissolved toxic substance; cyanide [40, 41] dimethyl sulfide [42], patricides [43] were reported.

The way to get the image results can rely on fluorospectrometry, which is the detection of fluorescence phenomena. Under the excitation of radiation, smartphones detect the light emitted by the target or fluorescence probe. The fluorescence quenching signals were monitored using the color pixel relationship, which was then utilized to quantify the relationship to concentration of target [44]. This method was frequently reported in immunoassay and with as biosensor [45-47]. As to be a spectrophotometer, smartphone was reported to be used for UV-spectrophotometry. Smartphones have been used to acquire spectra via diffraction gratings to disperse incoming transmitted light, before detection using the smartphone camera sensor [48]. This technique was applied for monitoring an absorption processing such as dye removal from wastewater [49, 50] and also in bioassay [51, 52]. In another way, smartphone camera can detect color change of sample directly with no need additional equipment (Filter or grating). This approach, called smartphone-based colorimetry, detects the sample's optical features typically over a broad range of wavelengths

when its structural shifts or plasmon resonance phenomena occurred [53]. The image color was interpreted to color pixels and then investigated the relationship to the concentration of an analyte under an expressing reaction including chemical reaction and bioassay reaction [54, 55].

2.3 SMARTPHONE BASED COLORIMETRY

Smartphone is used to be a color detector by using camera sensor. Figure 2 shows a draft summary of the process. After color generated, it is captured by smartphone camera in an appropriate environment. The image will be translated to color value, and the most suitable mathematical relationship is then discovered.
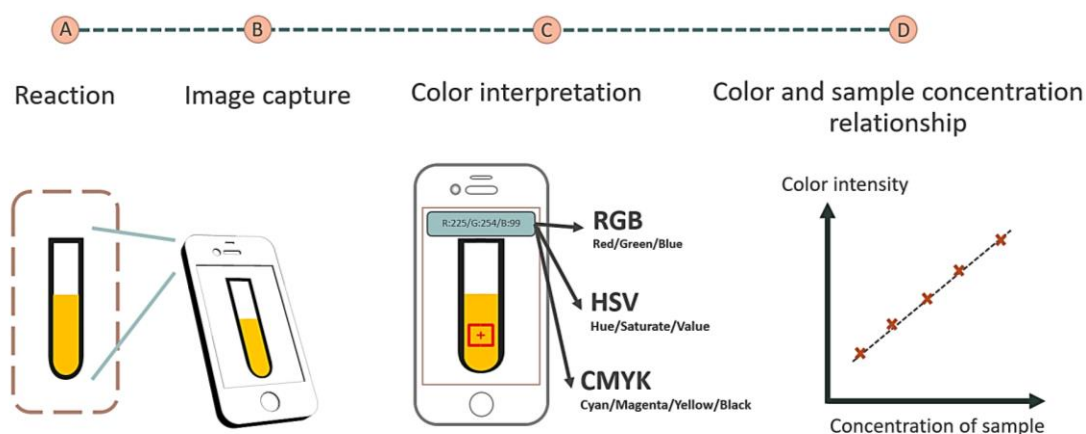
Figure 2. Flowchart of colorimetry using smartphone as a color detector.

2.3.1 Image acquisition

To get the image, there are main composition including sample, light and image sensor.

2.3.1.1 Interesting object or sample

Currently, colorimetry based on digital images acquired by smartphone cameras has been employed for the assays of various substances in various platform such as a solution in cuvette [56], solution in microwell [57] or in a solid phase e.g., paper-based assays [37, 40, 58-60], thin layer chromatography [61, 62], and biological skin [63].

2.3.1.2 Light

Light is the most important factor for image capture, influencing color quality and consistency. The image sensor will detect the object through transmission and reflexion, similar to how human eyes work. LED, LCD screen and embedded flashlight of smartphone were reported to be a good choice [37, 57]. Moreover, to control light interference from outside, in-house box or 3D printing box were adapted and developed for this reason.

2.3.1.3 Image sensor (smartphone)

There are two main types of sensors used in smartphone i.e., CMOS and CCD. A smartphone camera image sensor is a component that converts the light entering the camera through the lens into a digital picture. A sensor's surface comprises millions of photosites, also known as pixels, which are responsible for light capture. Smartphone sensors do not see color by default. A color filter array is put across the photosites in color cameras to recreate the color information in the final digital image [64].

2.3.2 Color interpretation

2.3.2.1 Color system

A color system, also known as a color space, is a collection of colors that describe how colors are represented. Some systems explain by combining three or four primary colors. To determine the relationship between color and amount of substance, the color intensity of the interesting area is converted to a numeric color value that is classified in several color systems.

2.3.2.1.1 CIE system

CIE system is a popular basic model used to communicate color in the first of 20th century and still now, which was developed by The Commission International de l'Eclairage (CIE). It explains the component of color in XYZ dimensions. The colors in the system are created from three main lights at wavelength of 436 nm, 546 nm, 700 nm represented blue, green and red lights which called primaries [65]. In 1931, CIE represents the best perception similar with human eyes, call CIE 1931. And it was a model for any system after that, for

example, CIE L*a*b* etc. There hasn't been much reported on using the CIE system to quantitate the amount of sample [66]. Because the color value is calculated in a complicated manner and does not correspond to the color used on screen or in printing.

2.3.2.1.2 RGB color system

The RGB color system is the most popular color system used for smartphone-based analysis [56, 63, 67-69] because it is a color system used in the sensor of a smartphone camera or represented on screen and display. The system consists of Red (R), Green (G), and Blue (B) primary colors (Figure 3A). Each color has a value in the range of 0 to 255. An expressed color consists of three primary colors in varying amounts. The black color is 0, 0, 0, and the white color is 255, 255, 255, representing red, green, and blue, respectively.
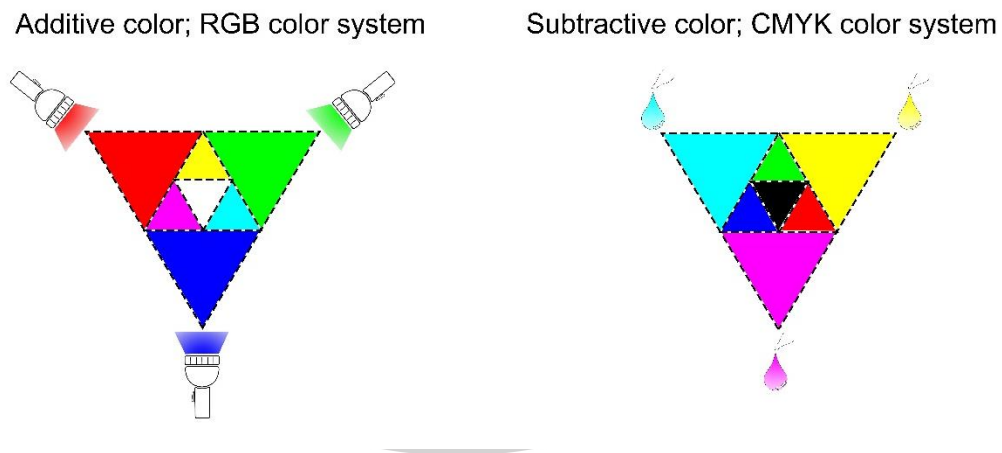
Figure 3. RGB (A) and CMYK (B) models.

2.3.2.1.3 CMYK color system

CMYK is subtractive color which be used for printer or dye. The main primary colors are Cyan (C), Magenta (M), Yellow (Y) and Key (K) or Black (Figure 3B). The values of them are 0-100%. This color system has not been frequently reported for smartphone-based analysis [70].

2.3.2.1.4 HSV color system

The HSV color system is a combination of three parts, which are hue (H), saturation (S), and value (V), or lightness, shown in a conical geometric shape [71]. Hue represents the shade of color in values of 0° to 360°. Saturation represents the intensity of color in values of 0 to 100% or 0 to 1. Lightness shows how dark a color is on a scale of 0 to 100% or 0 to 1, where 0 is the darkest or blackest and 1 is the lightest or white. Figure 4 shows the HSV color diagram. HSV is one of the most popular color systems used in smartphone-based analysis [72-75].
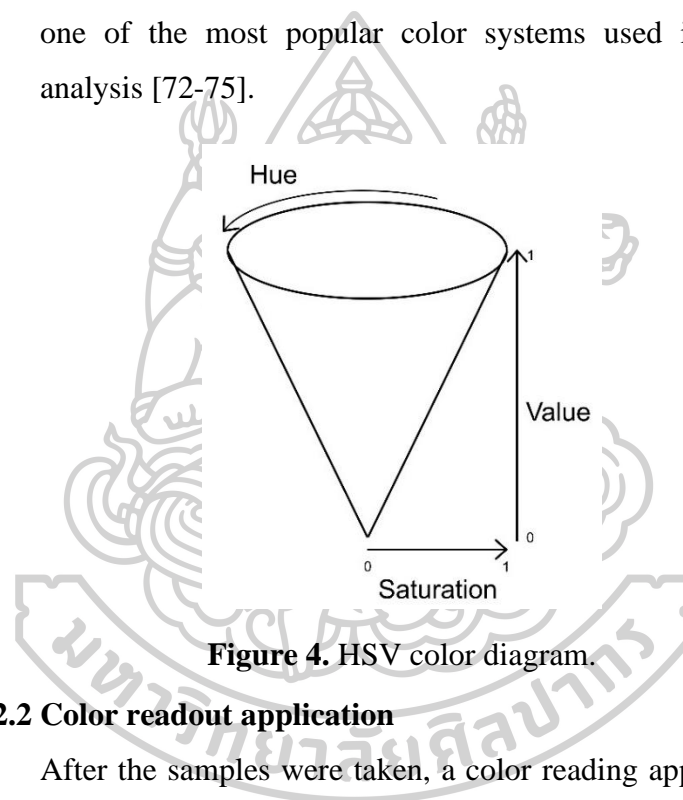
Figure 4. HSV color diagram.

2.3.2.2 Color readout application

After the samples were taken, a color reading application was used to convert the color of the image in the interested area into a digital number or color value.

2.3.2.2.1 Application on computer

To be interpreted on the computer or laptop, image needs additional step to transferred from smartphone or image capture device to computer. The application was used, for example ImageJ [69, 76] and Photoshops [77].

2.3.2.2.2 Application on smartphone

This method is more convenient than computer programs because of no data transfer, and it may be easier due to smartphone use easily. Commercial application on smartphone in both of Android and iOS system were used including Color Grab [78], Color picker [62], In-house applications [40].

Some applications can work starting from the capture process to data analysis and the result reporting by themself. There are both of commercial applications, which were published in online store and can be adapted with any sample, for example, MATLAB [56], Photometrix [79-81], and In-house applications, which were developed by the user. Its benefits are specific to sample and demand of result and can adjust easily [34, 36, 68].

2.4 SMARTPHONE-BASED METHOD IN PHARMACEUTICAL ANALYSIS

Smartphone was used for a quantitation in many fields as mentioned previously including in pharmaceutical field. Varity of drugs were assayed including anti-histamine drug; levocetirizine [68], NSAIDs; ibuprofen [2], sulfadiazine and sulfasalazine [1], antiviral and antibiotic; emtricitabine in bulk and tablet dosage form [80], cephalexin [82], tetracycline [83], chloramphenicol [84], carbamazepine, ciprofloxacin, norfloxacin [76], and ofloxacin and ornidazole [62]. Moreover, smartphone can play a role over the quantitating tool in pharmaceutical care by serving as a device for improving the healthcare service system [85, 86] and operating the 3D printer at the point-of-care for personalized medications [87].

2.5 REACTION IN PHARMACEUTICAL ANALYSIS

Many reactions employed in pharmaceutical analysis showed the potential to be adapted to smartphone-based analysis, however this thesis focused on three reactions.

2.5.1 Simple colorimetry based Ellman's assay

The simple colorimetry is a color measurement method in which the reaction does not require many components. It might be as simple as two or more compounds

reacting directly in a medium to generate a color. The color of reaction can be measured to the absorbance by spectrophotometry in which it is proportional to the concentration of a solute (Figure 5).

A (colorless) + B (reagent)→ C (color) + D
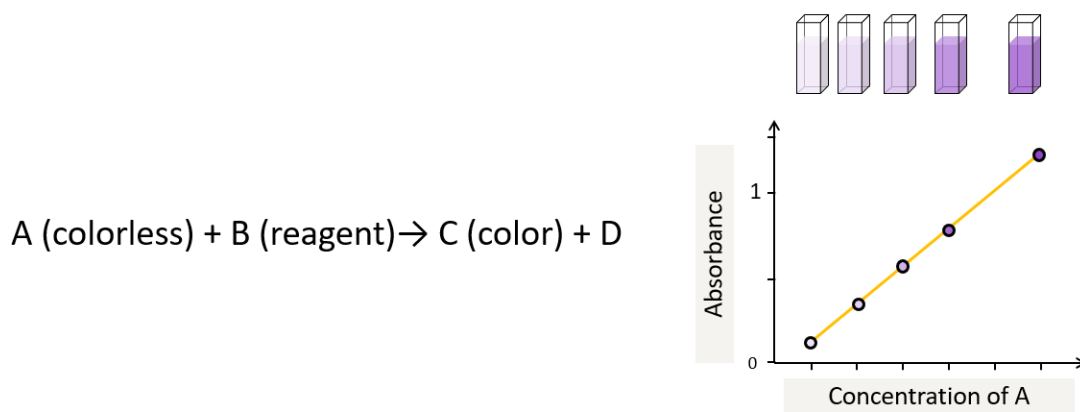
Figure 5. Common equation for direct colorimetry and relationship of substrate concentration and color signal.

2.5.1.1 Ellman's reaction

Ellman's reagent or 5,5′-dithiobis (2-nitrobenzoic acid), known as DTNB, is commonly known and used for quantifying free sulfhydryl groups and produce a yellow-colored product, named 2-nitro-5-thiobenzoic acid (TNB), which can be detected by spectrophotometry at wavelength of 412 nm. Figure 6 shows the equation of Ellman's reaction. Various compounds were tested using Ellman's technique, including cysteine in protein [88], glutathione and homocysteine in plasma [89, 90] and sulfhydryl groups in thiolated polymers [91-93].
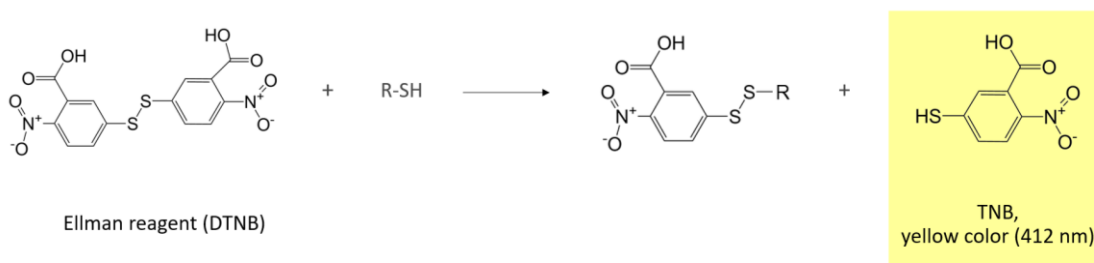
Figure 6. Ellman's reaction.

2.5.1.2 Thiol compound samples

Free thiol group can be detected by various techniques, for example, colorimetry (using Ellman's reagent), RP-HPLC [94], or thiol adduct with different detection method e.g., fluorescent spectrometry [95], mass spectrometry [96]. However, Ellman's reagent is a classical chromogenic reagent for thiol detection.

2.5.1.2.1 D-penicillamine

D-penicillamine is a pharmaceutically essential thiol-containing molecule that is used to treat a variety of illnesses including cystinuria, liver disease, rheumatoid arthritis, heavy metal toxicity, and Wilson's disease [97]. Figure 7 shows D-penicillamine structure. For the determination of D-penicillamine in pharmaceutical preparations, several approaches have been used such as UV–visible spectrophotometry [5-7], fluorospectrometry [8, 9], HPLC [10], flow injection analysis [11], capillary electrophoresis [12], etc.
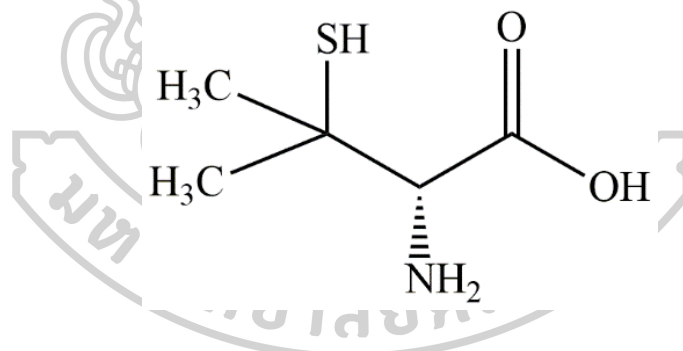
Figure 7. D-penicillamine structure.

2.5.1.2.2 Cysteine conjugated chitosan

Cysteine conjugated chitosan is a thiol containing polymer which improve mucoadhesive properties of chitosan used for drug delivery. Thiol group on the modified polymer interacts with mucus with a stronger bonding; disulfide bond, to maintain drug at side of action [92, 93, 98, 99]. Figure 8 shows cysteine conjugated chitosan structure. There has been no record of Ellman's reagent interacting with this polymer.
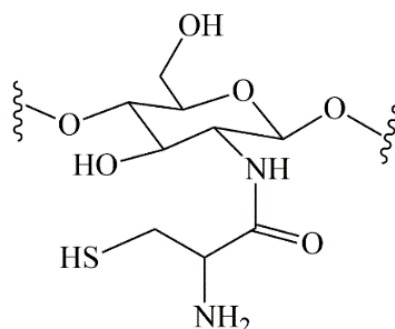
Figure 8. Cysteine conjugated chitosan structure.

2.5.2. Ion-pair extraction

Extraction is a method that has been used for a long time. Liquid-liquid extraction is a basic and well-known method. Ion pair extractive spectrophotometry is a sort of analytical technique created from the combining of colorimetry and liquid–liquid extraction. In this approach, the analyte forms a neutral ion pair complex with an oppositely charged ion pair reagent by charge transfer or electrostatic interaction, which can then be extracted using an organic solvent, and the extract is further analyzed. In the case that an organic dye is used as an ion pair reagent, it is very useful for the colorless analyte with low absorption to make the analyte quantifiable in the visible range and measurable by the measurement of the absorbance [100]. Figure 9 shows ion-pair extraction graphic.
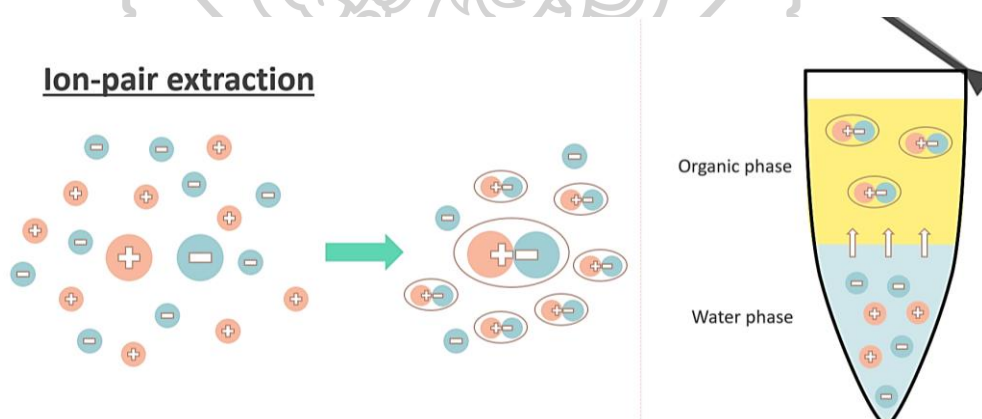
Figure 9. Ion-pair extraction graphic.

Ion pair extractive spectrophotometry has been applied to routine analytical and quality control assays of various drugs, e.g., desloratadine [96], losartan [101], levofloxacin [102, 103], ampicillin [104], and amoxicillin [105]. The approaches provide adequate selectivity, sensitivity, accuracy, and precision; nevertheless,

important disadvantage remain. The isolation and transfer of the organic phase during repeated extraction, dilution, and absorbance measurement may expose analysts to hazardous solvents, such as chloroform [101, 103, 105-107] and dichloromethane [102, 104]. Back-extraction of ion pair complexes into the aqueous phase can be done to decrease the danger of exposure to hazardous solvents. However, this requires time-consuming processes and can lead to sample loss. Aside from that, some previously published techniques employ a substantial quantity of organic solvent, which raises the cost of analysis and causes harmful waste to be released into the environment.

2.5.2.1 Developed method for ion-pair extraction

Small-scale ion-pair extraction was developed to solve the environmental issue as well as the human hazard. A mini-scale ion pair extractive assay for chlorpheniramine maleate was published, with the amount of organic extractant utilized limited to 500 μL per sample [15]. Nonetheless, the process was designed for the organic phase to be transferred. Furthermore, measuring the absorbance of a few microliters of the aqueous phase following back-extraction necessitates the use of a drop-based spectrophotometer, which is not a common equipment in chemical laboratory.

Smartphone was reported in a few work that was used in the extraction and analytical process, generating color from the ion-pair formation under the suitable environment [35, 78]. The experiments showed no phase isolation and loss of the extract before measurements, in which the risk of solvent contact was reduced. Moreover, the recent updates showed higher photographic performance by taking photo more than one analyte per shot [38, 108, 109]. The analysis of multiple samples was time-cost effective and reduces shot-to-shot variations. So, in this work, the smartphone-based colorimetry was developed for analyze multi-samples simultaneously without phase transfer.

2.5.2.2 Compound sample

2.5.2.2.1 Chlorpromazine hydrochloride

Chlorpromazine hydrochloride (CPZ) is an antipsychotic medication that is used to treat a variety of mental and emotional

problems. It is a basic drug with a pka of 9.3 that can be ionized at low pH. Figure 10 shows CPZ structure. Given that the current assay for CPZ tablet, according to the United States Pharmacopeia (USP43) reference method, relies on liquid–liquid extraction in which the sample is extracted with four parts ether and four parts 0.1 N hydrochloric acid, it is time-consuming and conflicting with green chemistry. To determine the quantity of drug, the absorbance of the collected organic phase was measured at 254 and 277 nm using a UV spectrophotometer. Furthermore, various techniques for estimating CPZ in bulk and different dosage forms have been published, including HPLC [13, 110], potentiometry [111], nuclear magnetic resonance spectroscopy (NMR) [14] and flow injection analysis [112], require sophisticated and expensive instrumentation.
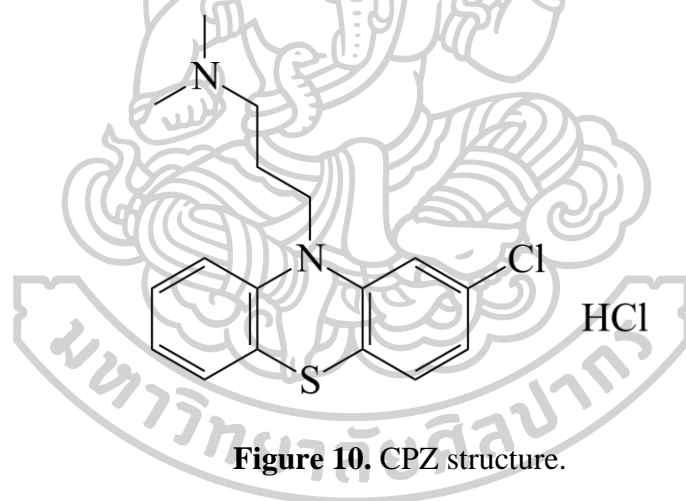
Figure 10. CPZ structure.

2.5.3. Titrations

Titration is a typical procedure in pharmaceutical test that involves reacting an unknown sample with a known concentration chemical called a titrant. The moment at which two chemicals entirely react is known as an endpoint, and it may be detected by changes in signal, such as solution color, pH, and voltage. The titration method requires more than 1 mL of a substantial volume of solvent, sample, and titrant. Furthermore, some variations can be made easily by researchers, such as endpoint observation and reading of the final volume of titrant used. Although the number of smartphone-based assays based on the comparison of color pixels of samples to a standard curve has expanded greatly, a smaller number of smartphone-based

procedures coupled with titrations has been published. Titrations in such works were based on diverse chemical reactions and were carried out in a variety of sample containers, such as ordinary conical flasks [17], flow cells [16, 113, 114] or microplates [115]. In addition, several lab-on-paper titrations were developed as a spot test analysis to lower the consumption of reagents [116-118].

2.5.3.1 Type of titration curves

2.5.3.1.1 Sigmoidal curve

A sigmoidal curve is a common curve that is used to express the behavior of a signal that results from titration. The titration signals were plotted against the volumes of titrant used, which looked like an S shape (Figure 11A). Of all the smartphone-assisted titrations reported, the equivalence point was determined by the comparison of the color response with a calibrated reference [116, 118] or the calculation of the maximum of the first derivative or the zero of the second derivative (Figure 11B, 11C) from a sigmoidal titration curve [16, 115, 116].
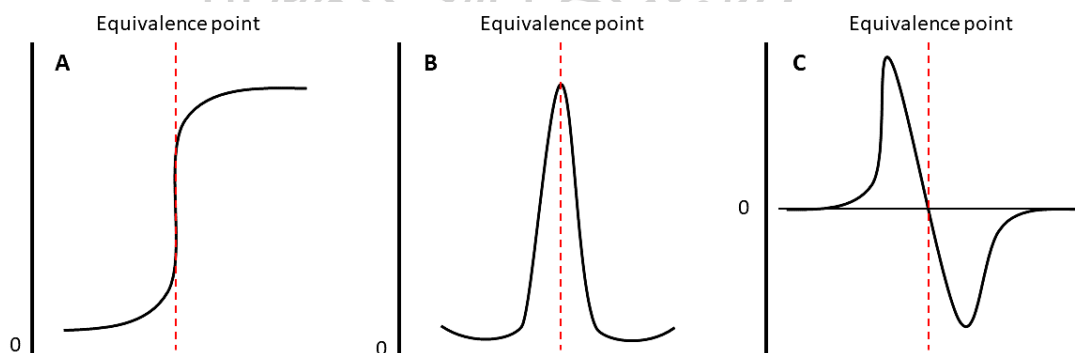
Figure 11. Sigmoidal curve (A) and its first (B) and second derivatives (C).

2.5.3.1.2 Linear-segment curve

Another curve is a plot of the titration signals against the volumes of titrant used that showed by two regions of linear line (Figure 12). The equivalence point is calculated from the intersection of those two lines. The linear segment curve is a titration curve that has

had little research done on it, and no smartphone-based approach for endpoint detection has been developed based on the usage of a linear segment curve.
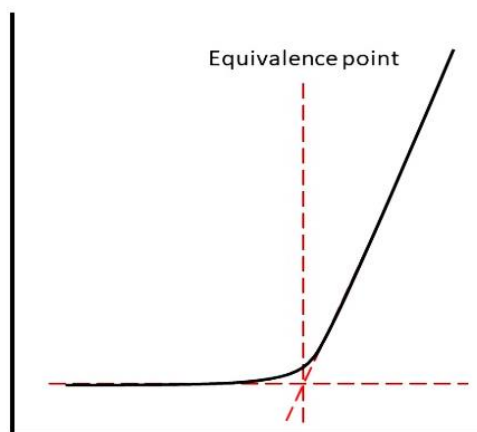
Figure 12. Linear-segment curve

2.5.3.2 Titration for chloride assay

2.5.3.2.1 Volhard' titration

Volhard titration is a back titration used for chloride detection. Silver ion (Ag^+) from silver nitrate ($AgNO_3$) reacts with chloride (Cl^-) in acidic environment and then silver chloride (AgCl) is precipitated, leaving unreacted silver ion in solution. Unreacted silver ion is titrated with known concentration ammonium thiocyanate (NH_4SCN) until Ag^+ run out of. Color of solution is change from clear to reddish orange when excess thiocyanate ion (SCN^-) reacts with ferric ion ($Fe3^+$) from ammonium iron(III) sulfate ($FeNH_3SO_4$) (Figure 13), mean that reaction is reached the endpoint.

$$Cl^- + Ag^+ \text{ (excess)} \rightleftharpoons AgCl \text{ (s)} + Ag^+ \text{ (unreacted)}$$

$$Ag^+ \text{ (unreacted)} + SCN^- \rightleftharpoons AgSCN \text{ (s)}$$
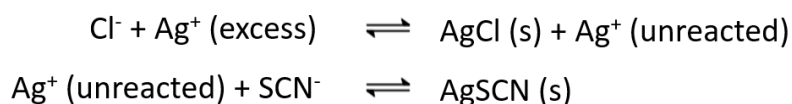
At the equivalence point; $\quad Fe^{3+} + SCN^- \rightleftharpoons FeSCN^{2+}$ (orange)

Figure 13. Volhard's reaction equation

2.5.3.3 Compound sample

2.5.3.3.1 Sodium chloride injection

Sodium chloride injection is a source of electrolyte and water for low salt syndrome or hydration. Sodium is the most abundant cation in extracellular fluid, regulates water transport, fluid balance, and osmotic pressure in bodily fluids. In the management of the acid-base equilibrium of body fluid, sodium is also linked to chloride and bicarbonate. Chloride is the primary extracellular anion, closely follows sodium metabolism, and changes in chloride concentration indicate changes in the body's acid-base balance. Table 1 shows smartphone-based method reported for chloride assay.

Table 1. Comparison of smartphone-based methods reported for the determination of chloride

Method	Technique	Sample	Material required	Analytical range (mM)	Reference
Colorimetry based on the reaction with gold nanoparticles on paper device	Comparison of color shade on test strip with color comparative wheel	Seawater, estuarine water	- Gold nanoparticles - Wax-patterned paper - Color comparative device	86–684	[119]
Colorimetry based on the reaction with silver nitrate and potassium chromate	Comparison of RGB signal with a calibration curve	Raw milk	- 3D-printed chamber containing white LED and video camera	3–99	[81]
Fluorometry based on the reaction with citric acid-cysteine sensor	Comparison of fluorescence intensity with a calibration curve	Sweat	- Citrate-based fluorescent sensors - 3D-printed device with excitation light from UV-LED lamps	0.8–200	[120]

CHAPTER 3
MATERIALS AND METHODS

3.1 MATERIALS

- 5,5'-dithiobis (2-nitrobenzoic acid) (Ellman's reagent or DTNB) (Sigma-Aldrich, USA)
- 96-well Microplate (Corning®, Corning Incorporated, USA)
- Ammonium thiocyanate (Ajax Finechem, New zealand)
- Ammonium iron(III) sulfate (Carlo Erba Reagents, France)
- Chlorpromazine hydrochloride (Sigma Aldrish, USA)
- Commercial 0.90% and 0.45% Sodium chloride injections (Thainakorn, Thailand)
- Chloroform (ACI Labscan, V.S.CHEM HOUSE, Thailand)
- Disodium hydrogen orthophosphate (Fisher Scientific, UK)
- Dichloromethane (Merck, Germany)
- Diethyl ether (Merck, Germany)
- D-penicillamine (≥99.0%) (Sigma-Aldrich®, Germany)
- D-penicillamine disulfide (Sigma-Aldrich®, Germany)
- Ethyl acetate (QReC ™ New Zealand)
- L-cysteine hydrochloride monohydrate (≥ 98.0%) (Sigma-Aldrich, USA)
- Methanol
- Methyl orange (Sigma Aldrish, USA)
- N-amyl acetate (Sigma Aldish, USA)
- N-butyl acetate (Carlo Erba Reagents, France)
- Nitric acid (EMSURE, Merk, Germany)
- Potassium hydrogen phthalate (Carlo Erba Reagents, France)
- Sodium chloride (Sigma Aldrish, USA)
- Silver nitrate (VWR, Belgium)
- Sodium citrate (Carlo Erba Reagents, France)
- Sodium dihydrogen orthophosphate (UNIVAR, APS, Australia)

- Low retention tip 200 µL, 1000 µL (Eppendorf AG, Germany)
- Microcentrifuge tube 1.5 mL (SPINWINTM, Tarsons, India, AXYGEN, China)
- Microcentrifuge tube 2 mL (AXYGEN, China)
- Polylactic acid filament for 3D printing (Shenzhen eSun Industrial Co., Ltd., China)

3.2 EQUIPMENT

- Analytical balance (SARTORIUS AG Gottingen, Germany)
- Autodesk 123D Design (version 2.2.14.0, Autodesk Inc.,US)
- C18 HPLC column (4.6 x 150 mm, 4.6 x 250 mm, 5 µm; Cosmosil® Japan)
- Fused Deposition Modeling (FDM) 3D printer (Prusa i3 MK3, Czech Republic)
- HPLC machine (Agilent 1260 Series, Agilent Technologies, Germany)
- Huawei (Nova 3i, Huawei Device Co., Ltd., Chaina)
- ImageJ software (National Institute of Health, MD, USA)
- iPad (5th generation, Apple Inc., US)
- iPhone (5s, 11, Apple Inc.,US)
- Microcentrifuge machine (Microfuge® 16 Centrifuge, BECKMAN COULTER)
- Micropipette 2-20 µL, 20-200 µL, 100-1000 µL (Eppendorf Research®, Eppendorf, Germany)
- Microplate reader (Victor Nivo TM Multimode plate reader, PerkinElmer, UK)
- pH meter (LAQUAtwin pH, HORIBA, Japan)
- Samsung (A5, Galaxy Note 9, Galaxy S20+, Samsung, Korea)
- Shaker (Multi-spin, Biosan, Latvia)
- UV-Visible spectrophotometer (Cary 60 UV-Vis, AGILENT TECHNOLOGIES, Malaysia)
- Vortex (VX100, Labnet International Inc., USA)

3.3 METHODS

3.3.1 Development of smartphone-based Ellman's assay

The Ellman's reagent was performed with D-penicillamine solution directly in a 96-well microplate and then the image was captured by a smartphone from the top view in a light-controlled box. The color intensity was readout into RGB values by using a commercial mobile application. The standard curve was plotted between drug concentration and color values through an appropriate mathematical transformation. Finally, a drug sample's concentration was determined.

3.3.1.1 Preparation of D-penicillamine and Ellman's reagent solution

Standard stock solution was prepared by weighing D-penicillamine accurately and dissolving in 1 g/L EDTA solution. The solution was then diluted using the same solvent to obtain a series of working solutions at 5, 10, 20, 30, and 40 µg/mL. Ellman's reagent solution was prepared by weighing Ellman's reagent accurately and dissolving in 0.1 M sodium phosphate buffer, pH 8.0.

3.3.1.2 Procedure of Ellman's reaction

To make the reaction, 150 µL Ellman's reagent solution was mix with 150 µL of standard or sample solutions in a 96-well, flat-bottom transparent microplate to form a yellow 2-nitro-5-thiobenzoic acid (TNB) product. The blank was prepared in the same manner using distilled water instead of D-penicillamine solution. After 10 min, the plate was captured.

3.3.1.3 Procedure of digital image capture and color acquisition

The 96-well microplate containing sample was placed on the iPad screen (5th generation) which was a light source and an image was captured by the back camera of the smartphone (iPhone 5s) in the light-controlled box though a punctured hole on the top of the box at a distance between the plate and camera aperture of 20 cm (Figure 14). The camera was set in the automatic focus mode with the flash turned off. From the image, which was saved as a JPEG, the color intensity was measured by using a color reader mobile application, namely Color Name AR (version 2.0).
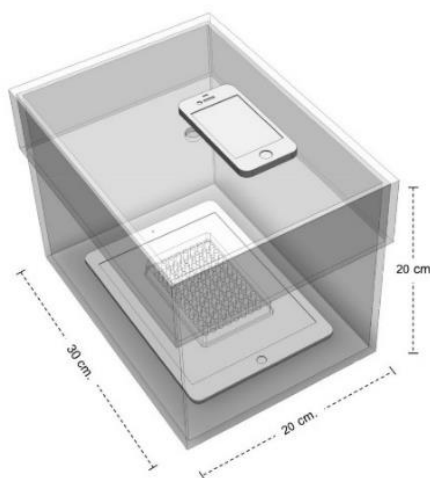
Figure 14. Image capture setting of smartphone-based Ellman's assay.

The color intensity was translated into R, G, and B values, and these values were plotted against different penicillamine concentrations ranging from 5 to 40 µg/mL in order to find out the relationship between the R, G, and B values and the drug concentration. A mathematical transformation of color pixels was studied to discover the best relationship between them, which was considered from the r-square of linear regression.

3.3.1.4 Optimization of reaction

Factors including concentration of Ellman's reagent (0.3–1 mM) and time of reaction (10–30 min) were studied. The reaction was performed by analyzing the standard solution in range of 5–40 µg/mL with pH controlling at 8.0, following originally method conducted by Ellman [121]. After reaction was produced, the image of result solutions was captured by smartphone under procedure in section 3.3.1.3 and color values were then interpreted. The parameters derived from linear regression of standard solution i.e., r-square and slope were considered to choose the best condition.

3.3.1.5 Optimization of image acquisition and color interpretation

3.3.1.5.1 Sample array

The reaction was performed in 50-mL centrifuge tube by mixing 15 mL of Ellman's reagent solution and 15 mL of 25 µg/mL D-penicillamine solution. Then, 300 µL of solution was aliquoted into

96-well microplate and image was captured by smartphone following procedure mentioned in section 3.3.1.3. A relative standard deviation (%R.S.D.) of color value in different area size (4x4, 5x5, 6x6, 7x7, 8x8 well x well) was reported.

3.3.1.5.2 Type of smartphone

The standard curve of penicillamine was performed under the validated condition. The image of samples was captured by different smartphone brands, i.e., iPhone 5s, Huawei Nova 3i, and Samsung Galaxy Note 9. The slope, y-intercept, and r-square of the results were compared. If these elements were unrelated, each factor could be subjected to a proper mathematical transformation. After that, the concentration of penicillamine in the sample was estimated and recalculated.

3.3.1.5.3 RGB analysis tool

To study the effect of color reader application on smartphone, four applications from two operating systems (iOS and Android) were investigated. The images of penicillamine standard solution captured by the iPhone 5s were used to compare the impact of various mobile applications. The image was examined on the iPhone 5s, which represents an iOS mobile application (Color name, Pixel picker) and then uploaded to the Samsung Galaxy Note 9 to be analyzed, which represents an Android mobile application (Color grab, RGB color picker). The experiment was performed triplicate. The slope, y-intercept, and r-square of the results were compared.

3.3.1.6 Validation of method

The optimal method was validated following the ICH guideline in the issues including accuracy, precision, specificity, linearity, range, limit of detection (LOD), and limit of quantitation (LOQ).

3.3.1.6.1 Accuracy

Three concentrations of standard penicillamine were prepared at 80%, 100%, and 120% of the target concentration (25 µg/mL) and

analyzed by being spiked into the sample matrix or test sample, in cases where all expected components were impossible to reproduce. The test was performed three times per concentration. The %recovery was reported.

3.3.1.6.2 Precision

The sample was prepared at 100% of the target concentration and analyzed with six replicates. To confirm that the procedure is intended to be used, the analysis was performed repeatedly for three consecutive days. %R.S.D. was reported.

3.3.1.6.3 Linearity and range

Five concentrations of standard penicillamine were prepared across the range of analytical procedure and then the standard curve was performed under the validated condition.

3.3.1.6.4 Specificity

Some of the ingredients for penicillamine capsules, including silicon dioxide, magnesium stearate, and lactose, were chosen to be investigated, and penicillamine disulfide, which was an impurity in this preparation, was studied. The known amount of penicillamine standard was mixed with each ingredient separately in the percentage of the commonly used amount in the capsule. Then the mixtures were filtered and aliquoted to react with Ellman's reagent. The result was reported in %recovery.

3.3.1.6.5 Limit of detection (LOD)

LOD was calculated based on the standard deviation of the response and the slope. LOD was expressed as: $LOD = \dfrac{3.3\,\sigma}{S}$

where σ = the standard deviation of the response

S = the slope of the calibration curve

3.3.1.6.6 Limit of quantitation (LOQ)

LOQ was calculated based on the standard deviation of the response and the slope. LOQ was expressed as: $LOQ = \dfrac{10\,\sigma}{S}$

where σ = the standard deviation of the response

S = the slope of the calibration curve

3.3.1.7 Comparing the smartphone-based method to the conventional method for penicillamine capsule assay

To assay the drug contents in the capsules, the sample solutions were prepared following the procedures described in the USP43 [10] under Assay of Penicillamine Capsules. Briefly, after ten capsules were carefully opened, the contents and the empty capsule shells were transferred into a 2 L-volumetric flask. The EDTA solution (1 g/L) was added to dissolve the contents, then the mixture was allowed to stand at room temperature for 90 min. The resulting solution was filtered through a 0.45-µm syringe filter and diluted to the appropriated analytical concentration (middle of standard curve). Finally, the sample solutions were analyzed by high performance liquid chromatography (HPLC) following the condition in Table 2. The obtained % labeled amount (%LA) was compared with the smartphone-based result, which was analyzed under the optimal condition.

Table 2. Chromatographic conditions for assay and dissolution test of penicillamine capsule

	Assay	Dissolution
Dissolution parameters		
Medium	-	0.1 N HCl; 900 mL
Apparatus	-	1; 100 rpm
Sampling time	-	30 min
HPLC parameters		
Mobile phase	6.9 g/L of monobasic sodium phosphate and 0.2 g/L of sodium 1-hexanesulfonate in water	Methanol and Buffer solution (3:97)
Column	4.6-mm × 25-cm; 5-µm packing L1	4.6-mm × 15-cm; 5-µm packing L1
Detector	UV 210 nm	UV 210 nm
Flow rate	1.6 mL/min	1.0 mL/min
Injection volume	20 µL	30 µL

Besides being used for the assay, the developed method was applied to the determination of the amount of drug released in the dissolution test of penicillamine capsules. The sample solution was withdrawn 10 mL from each vessel, for a total of six vessels, after 30 min of testing, and then filtrated and analyzed by HPLC condition showed in Table 2. From the same sample solution, it was tested by the optimal smartphone-based method and UV-vis spectrophotometry using microplate reader at wavelength of 412 nm. The % drug release from these methods were compared.

3.3.1.8 Comparing the smartphone-based method to the conventional method for the analysis of thiol group in thiolated polymer

To extend the application of smartphone as a color detector and translator for Ellman's reaction, free sulfhydryl (-SH) groups in a thiolated polymer was quantified. A cysteine-conjugated chitosan was used as a sample polymer in this study. For this purpose, 10 mg of the polymer was dissolved in

500 µL of 0.1 M potassium phosphate buffer, pH 8.0 and a standard curve of cysteine in the range of 5–40 µg/mL was created. The Ellman's reaction was carried out following the procedures described in Sahatsapan et al. [92]. Briefly, 500 µL of Ellman's reagent was mixed throughout with 500 µL of sample or standard solutions in 1.5 mL microcentrifuge tube and the reaction was allowed to proceed for 2 h. Subsequently, the mixture was diluted to an appropriate concentration. Three hundred microliter of solution was aliquoted into 96-well flat-bottom transparent microplate to be analyzed with microplate reader (Victor Nivo^{TM} Multimode plate reader) at 412 nm and captured by smartphone camera. Amount of free sulfhydryl groups (µmol) per gram polymer was calculated and compared.

3.3.2 Development of smartphone-based ion-pair extraction

The ion-pair extraction of chlorpromazine hydrochloride (CPZ) was performed in a microcentrifuge tube by using methyl orange (MO) to form ion-pair complex. The complex was extracted into more safe organic solvent and tubes containing 2-phase of organic and aqueous phase were arranged in a circular 3D-printed rack and captured from the top view of light-controlled box with a smartphone camera. The color intensity of the organic phase was converted to R, G, and B values using a mobile application. The standard curve was then plotted between color values, through an appropriate mathematical transformation, and drug concentration.

3.3.2.1 Preparation of standard and sample solution

Fifty milligrams of CPZ standard were dissolved in 20 mL water to obtain a 2.5 mg/mL stock solution. Subsequently, a series of working standards were prepared by diluting the stock solution with water to the final concentrations of 2.5–50 μg/mL.

The sample solution was prepared by weighing and grinding 10 CPZ tablets to fine powder. A portion of the tablet powder containing 100 mg CPZ was accurately weighed in a 50 mL volumetric flask, and 20 mL water was added. Afterward, the sample solution was sonicated for 15 min, adjusted to a certain volume with water, and filtered through Whatman's No. 1 filter paper.

The clear filtrate was further diluted with water to a final concentration of 25 µg/mL.

3.3.2.2 Procedure of ion-pair extraction

At a constant room temperature (25 °C), the ion pair extraction was conducted in a 1.5-mL polypropylene microcentrifuge tube by adding 100 µL of 0.2 M potassium hydrogen phthalate buffer, 400 µL of standard or sample solution of CPZ, organic solvent, and 100 µL of MO solution. Four hundred microliter of distilled water was used instead of the CPZ standard as a blank. Afterward, the mixtures were vigorously mixed using a vortex mixer and then centrifuged at 12,000 rpm for 1 min to separate the liquid phases. Finally, the yellow color in the organic phase was analyzed.

3.3.2.3 Optimization of ion-pair extraction

To discover the best conditions for extraction, four factors were studied, including pH of reaction (pH 2–8), concentration of MO (0.2–2 mg/mL), type of organic solvent, volume of organic solvent (500–800 µL), and time of reaction (30–240 s). When one factor was studies, other factors were fix. After the extraction of standard solutions at 2.5, 5, 10, 25, and 50 µg/mL, the organic phase of each concentration was transferred into a 96-well microplate and the absorbance was measured at 415 nm. A standard curve was constructed by plotting the relationship between the absorbance (Y-axis) and the concentrations of CPZ (X-axis) to compare the linear regression elements of each factor. The absorbance value and slope were compared in order to select the best condition to use in the following step.

3.3.2.4 Procedure for digital image capture and color interpretation

The organic phase and water phase were directly photographed while they stayed in the same microcentrifuge tubes. To enable a consistent and high-throughput image acquisition, an in-house 3D printed rack was fabricated to simultaneously photograph the multi samples in a single shot. The rack was placed on a clear glass sheet locked by a 3D printed adapter, 1.5 cm above the screen of the iPad (5th generation), which was used as a light

source (Figure 15). The image of extracts was captured through a small hole located at the top of a box using the back camera of a smartphone (iPhone 5s), using the automatic focus mode with the flash turned off. The color intensity was measured by using an iOS mobile application, namely Color Name AR (version 2.0), to be translated into R, G, and B values. They were plotted against CPZ concentrations to determine their relationship. A mathematical transformation of color value was investigated in order to find the best relationship by considering the r-square of linear regression.

Figure 15. Image capture setting of smartphone-based ion-pair extraction.

3.3.2.5 Optimization of image acquisition

3.3.2.5.1 Tube arrangement

The arrangement of tubes was studied in two alignments, radial and linear. The 25 µg/mL standard solution was extracted in a large scale by using the optimal condition of extraction, to produce a large volume of yellow-color phase from one extraction. The 1.4 mL of organic phase was transferred into 24 tubes of 1.5-mL microcentrifuge tube. The color variation in the organic phase was studied and compared between the two arrangements.

3.3.2.5.2 Luminous intensity of light source

The 25 µg/mL standard solution was extracted in a 1.5-mL microcentrifuge tube under optimal condition. Then, four levels of full brightness were set at 25%, 50%, 75%, and 100% while the image of

extracted tube was captured. The experiment was done in triplicate. The average color intensity was used to compare the results.

3.3.2.5.3 Tube turbidity

Due to differences in laboratory equipment, the properties of the tube may affect the color quality. As a result, two different levels of tube turbidity were investigated. The set of standard and sample solutions were extracted in a clear-wall tube and turbid-wall tube and captured under the optimal condition. The %LA of the samples contained in two types of tube were compared.

3.3.2.6 Validation of method

The optimal method was validated following the ICH guideline in the issues including accuracy, precision, specificity, linearity, range, limit of detection (LOD) and limit of quantitation (LOQ) following the same procedure mentioned in the previous section (section 3.3.1.6).

3.3.2.7 Comparing the smartphone-based method to the conventional method for CPZ tablet assay

The traditional method for the CPZ tablet assay was mentioned in USP43 [10]. To extract the sample, 10 mg of sample solution were mixed with 20 mL water, rendered alkaline with ammonium hydroxide, and extracted with four 25-mL portions of ether. After that, the combination of ether extracts was extracted back to the aqueous phase by four 25-mL portions of 0.1 N hydrochloric acid in a 250-mL separatory funnel. Finally, the four portions of aqueous extracts were collected in a 250-mL volumetric flask, adjusted to the volume with hydrochloric acid, and the absorbance was measured at wavelengths of 254 and 277 nm using a UV spectrophotometer. The %LA from the USP method was compared to those obtained from the smartphone-based methods.

3.3.3 Development of smartphone-based titration relying on Volhard's method

The sodium chloride solution was reacted with excess silver nitrate ($AgNO_3$) in a 2-mL microcentrifuge tube, and then the clear supernatant was divided into 9

tubes of 1.5-mL microcentrifuge for back titration with ammonium thiocyanate (NH$_4$SCN). The different titrant volumes were added to each tube. By that, the volume of titrant used had to cover the equivalence point in 4 points of colorless region and 5 points of color region, representing the region of before and after equivalence point. The centrifugation was then performed, and the supernatant from 9 tubes were transferred into a 96-well microplate and the image was captured by the smartphone. The RGB values were read using an Android mobile application. The equivalence point was calculated from the intersection of two lines in the linear segment curve, which was plotted between color intensity through an appropriate mathematical transformation and the added volume of NH$_4$SCN. The concentration of the sample was then calculated.

3.3.3.1 Procedure of standard solution preparation and Volhard titration

Weighing precisely 4.5 g of NaCl into a 500-mL volumetric flask and adjusting to volume with water yielded a 0.90% w/v NaCl solution. The Volhard's reaction was performed by mixing 550 µL of the NaCl solution, 100 µL of 6 N nitric acid, 100 µL of 5% ferric alum, and 960 µL of 0.1 N AgNO$_3$ together for 10 s. Then it was centrifuged for 5 minutes to precipitate AgCl. To get to the equivalence point, 180 µL of the supernatant was aliquoted into 1.5-mL microcentrifuge tubes for 9 tubes and titrated by a series of volumes of NH$_4$SCN. However, before the titration, the estimated equivalence point was calculated from the volume and the concentration of reagent to set the range of the NH$_4$SCN volume to be across the estimated equivalence point by covering 4 points before and 5 points after. Finally, the series of solutions were centrifuged, and 180 µL of the supernatants were aliquoted into a 96-well microplate for photography.

3.3.3.2 Procedure for digital image capture and color interpretation

The 96-well microplate containing the sample was placed on the tablet screen (Samsung S6 Tab, South Korea), which was a light source, and was captured by the back camera of Samsung Galaxy S20+ smartphone (Samsung, South Korea) in the light-controlled box through a small hole on the top of the box at a distance between the plate and the camera aperture of

20 cm (Figure 16). The camera was set in the automatic focus mode with the flash turned off. R, G, and B values were interpreted by an Android mobile application, namely "Color Detector" developed by Raimon Gaspar Fernandez, and plotted against different added volumes of NH_4SCN in order to find out the relationship between them. A mathematical transformation of color values was performed to find the most suitable regression between the volume of titrant and color values, which was considered from the r-square of the linear line. The equivalence point was calculated from the intersection of two lines derived from the colorless region and the orange region.
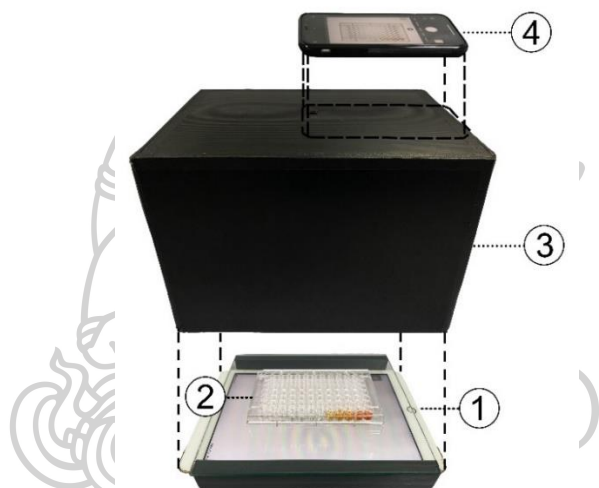
Figure 16. Image capture setting of smartphone-based Volhard's titration.

3.3.3.3 Optimization of image acquisition and color interpretation

3.3.3.3.1 Color of microplate wall

The influence of two colors of microplate wall on the color of the final solution was examined. The titration was carried out by evaluating 0.9% w/v of NaCl standard solution under optimal conditions in double volume of the typical reaction, after that the final solutions were aliquoted into clear-wall and black-wall microplates in the equal volume and the image was photographed using a Samsung Galaxy S20+. Finally, the equivalence points were then determined. The obtained titration curves and equivalence points were used to compare between clear-wall and black-wall microplate.

3.3.3.3.2 Type of light source

A tablet screen was tested and compared to an LED lamp to confirm the effect of different light sources. The titration of 0.90% w/v NaCl was performed in accordance with the best practice. The image of plate holding the titration solution was photographed using the tablet screen to be a light source, then transferred to another setting (Figure 17B) by using an LED lamp as a light source. The %LA of two methods was compared.
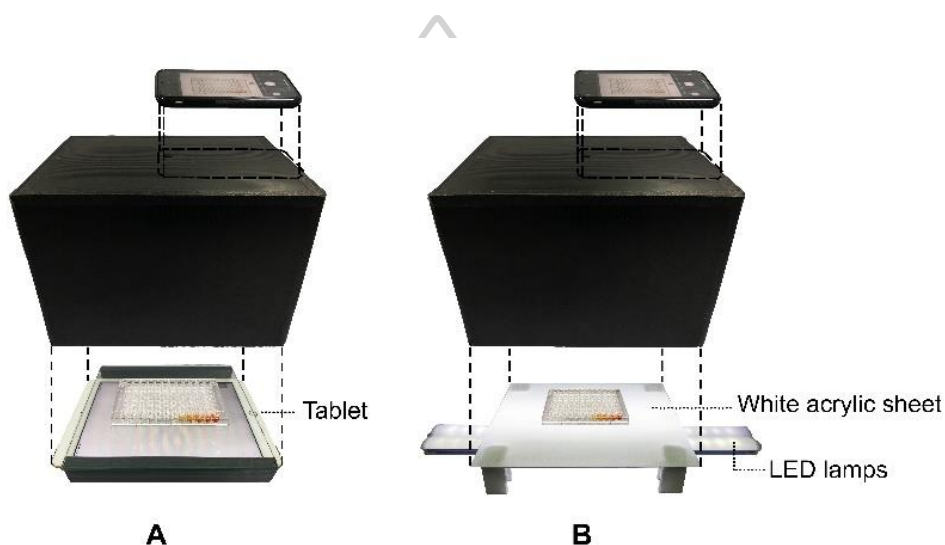
Figure 17. The image capture setting by using tablet (A) and LED lamp (B) as a light source.

3.3.3.3.3 Type of smartphone

The titration curve of 0.9% w/v NaCl was performed under the optimal condition. The samples were captured by different smartphone brands, i.e., iPhone 11 (iOS), Samsung Galaxy S20+ (Android), and Oppo Reno 3i (Android). The slope, y-intercept, and r-square of the results were compared. If these elements of three smartphone brand were unrelated, each factor could be subjected to a proper mathematical transformation. After that, the concentration of penicillamine in the sample was estimated and recalculated.

3.3.3.3.4 RGB analysis tool

The application on PC has been used in digital image colorimetry since the first era and still be used until now. ImageJ, a commonly used application was studied to compare with the applications on Android smartphone performed in this study. 0.9% w/v NaCl was assayed under the optimal condition. The image of titration results was captured and then interpreted to RGB values on the Samsung Galaxy S20+ using Color Detector application, which represents a mobile application and then uploaded to the PC to be analyzed by using the Color Histogram plugin, which represents a desktop program. The color signal of each point of titration curve were used to compare the impact of various mobile applications.

3.3.3.4 Validation of method

The optimal method was validated following the ICH guideline in the issues including accuracy, precision, linearity, and range. The ruggedness was studied by concerning when different analysts performed.

3.3.3.4.1 Accuracy

Three levels at 95%, 100% and 105% of 0.45% and 0.90% w/v NaCl were assayed under the optimal condition in triplicate and then the %recovery was interpreted.

3.3.3.4.2 Precision

The samples were examined at 0.45% and 0.90% w/v NaCl which were at 100% of the target concentration under the optimal condition and analyzed with six replicates and analyzed by three analysts. To confirm that the procedure is intended to be used, the analysis was performed repeatedly for three consecutive days. A %R.S.D. was reported.

3.3.3.4.3 Correlation of equivalence point and NaCl concentration

Ten levels of NaCl concentration in the range of 0.4163–0.9675 %w/v were examined using the optimal condition. The equivalence

points of each point were calculated and plotted against the NaCl concentration (%w/v). The r-square of linear regression was reported.

3.3.3.5 Comparing the smartphone-based method to the conventional method for NaCl assay

The validated method was applied for the assay of NaCl injection (0.9% and 0.45% w/v NSS) compared with the method described in the USP43 [10] and the previous method, UV-vis spectrophotometry [18]. The %LA results were compared between three methods. For the UV-vis spectrophotometry, the sample was tested in the same manner of the developed smartphone-based method. In the final step, the absorbance at 450 nm of the series of the resulted solution in 96-well microplate was measured. For the USP method, ten milliliters of 0.9 %w/v NaCl injection was added with 10 mL of glacial acetic acid, 75 mL of methanol and 3 drops of eosin Y. Then the mixture was titrated with 0.1 N silver nitrate to a pink end point.

3.3.4 Statistical analysis

Experiments were carried out in triplicate unless otherwise stated. All of the information was provided as a mean with a standard deviation (S.D.). The data were statistically analyzed using the analysis of variance (ANOVA) test and the Student's t-test, with a p-value of 0.05 declared significant. Microsoft[®] Office Excel 2010 was used to conduct all statistical tests.

CHAPTER 4
RESULTS AND DISCUSSION

4.1 DEVELOPMENT OF SMARTPHONE-BASED ELLMAN'S ASSAY

4.1.1 Selection of an appropriate RGB channel and data transformation

The color intensity of the sample was translated to R, G, and B values using a picture acquired by an iPhone 5s. These values were plotted against the penicillamine concentrations at 5, 10, 20, 30, and 40 µg/mL to investigate the relationship of R, G and B value and the drug concentration. With increasing penicillamine concentrations, the yellow color of the solutions increased while the intensities of B decreased exponentially (Figure 18A). The B value displayed the most noticeable change in intensity as a result of the drug concentration change, whereas the R and G showed minimal fluctuations. Hence, B was chosen for future analysis.
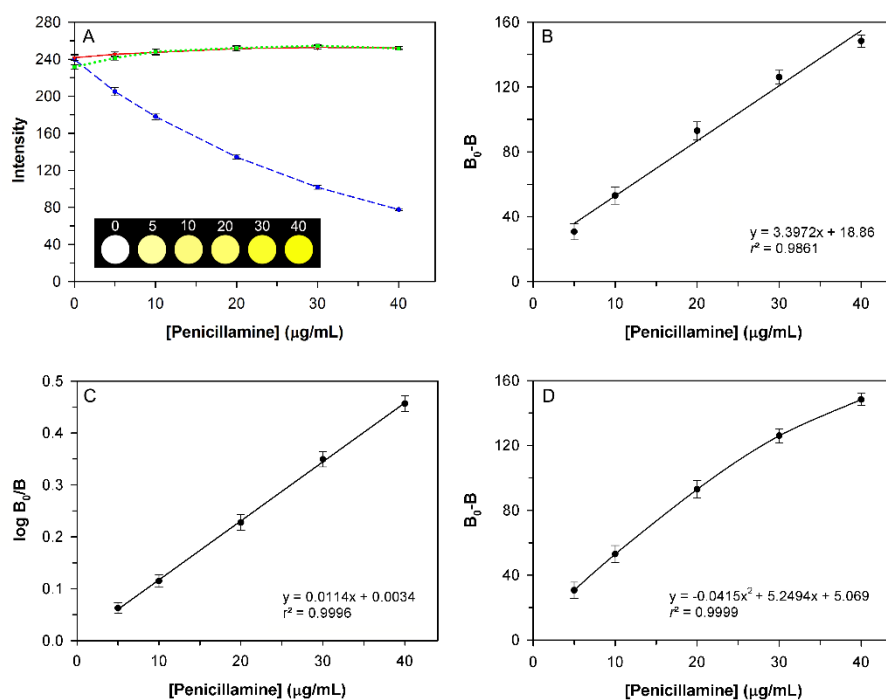
Figure 18. Plot of the penicillamine concentration versus Red (▼), Green (■), Blue (●) values and the yellow color of solutions (A). Plot of B value versus the penicillamine concentration; without data treatment (B), as logarithmic ratio (C) and using second-order polynomial regression (D).

In order to obtain the best-fitting model describing the relationship of color values to drug concentration, both raw color data [122-124] and suitably mathematical transformed data [37, 125] were presented in earlier works. In this investigation, converting B values to log B_0/B (where B_0 was the blank's B value) enhanced the relationship between analytical response and drug concentration substantially, giving a linear standard curve with a higher R^2 (Figure 18C) than that generated from untreated data (Figure 18B). Furthermore, untreated B values revealed a good non-linear correlation to the penicillamine concentration in a second-order polynomial regression model (Figure 18D). However, a linear relationship is more commonly used due to its simplicity for extrapolation. So, log B_0/B values were used for the creation of a standard curve for the assay in this study.

4.1.2. Optimal conditions for Ellman's assay

4.1.2.1 Concentration of Ellman's reagent

To get the best assay conditions, several parameters including the reaction time, Ellman's reagent concentration and photography condition were investigated. To keep stability to Ellman's reagent and assure the generation of TNB product in the intensely colored form, the reaction was performed at pH 8 using sodium phosphate buffer, as initially proposed by Ellman [121] and commonly used as a general procedure. The appropriate reagent concentration was studied for penicillamine in the concentration range of 5–40 µg/mL, and the findings were presented in Figure 19A. The use of 1 and 0.5 mM Ellman's reagent produced comparable equation describing the relationship between log B_0/B values (y) and penicillamine concentrations (x) with $R^2 > 0.9990$. However, using a lower reagent concentration (e.g., 0.3 mM) resulted in a slightly lower R^2 value due to a negative deviation at high analyte concentrations. As a result, 0.5 mM of Ellman's reagent was a suitable concentration to establish a good linear correlation between color values and drug concentration while also saving the reagent.
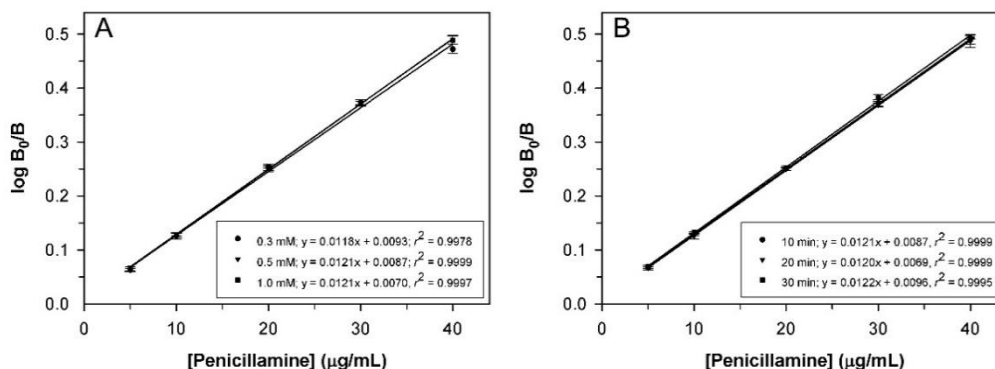
Figure 19. Effects of the concentration of Ellman's reagent (A); 0.3 mM, 0.5 mM, 1.0 mM and the reaction time (B); 10 min, 20 min, 30 min on the colorimetric reactions.

4.1.2.2 Reaction time

In terms of reaction time, there was no significant difference of the standard curves and the corresponding regression equations obtained from the different reactions proceeding at 10, 20 and 30 min, as shown in Figure 19B. Therefore, 10 min was chosen to finish the reaction with the least amount of time required. In addition, the findings of this investigation indicated that the color was constant for at least 30 minutes.

4.1.3 Optimal procedure for image acquisition and color interpretation

4.1.3.1 Sample array

In comparison to spectrophotometers, which are designed especially for signal measurement, smartphones' built-in cameras are easily impacted by light conditions and may produce incorrect analysis findings [126, 127]. To avoid influence from external light, the photography in this study was done by putting the samples in a dark box and directly lighting them with an iPad screen. Additionally, a distance of 20 cm was set between the smartphone camera and the microplate to avoid parallax error and achieve high precision and reproducibility. One issue was discovered since the light acquired by digital cameras are not precisely uniform across the field of vision, i.e., certain regions of the image, often the center near to the focus, are brighter while others are dimmer. From the current experiment, %R.S.D. of B values when interpreted in an area of 4x4, 5x5, 6x6, 7x7 and 8x8 well x well were 1.50,

1.87, 2.25, 2.56 and 3.25, respectively. It found that the same solutions that were in different wells gave varying color values at farther distances from the center (Figure 20). So, the samples should be located in a well array of less than 7 x 7 to minimize the inconsistency effect of color value by ensuring less than a 3% coefficient of variation is produced.
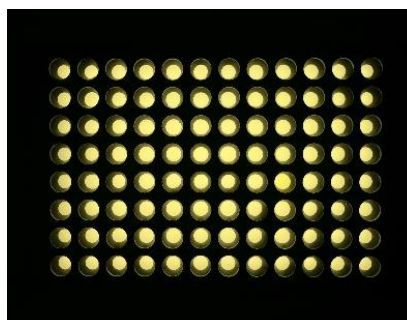
Figure 20. An image of a 96-well plate was captured at the center of the plate from the top view.

4.1.3.2 RGB analysis tool

Apart from the above-mentioned issues, the effect of different mobile applications used for RGB readouts were studied to find out the possibility of variation from different applications used. The B values interpreted from four RGB reader applications on the iOS and Android operating systems were utilized to generate penicillamine standard curves from the same iPhone-captured image. Table 3 shows that the values of the slope, y-intercept, and R^2 of the linear regression equations produced from different applications had no significant difference with p-value > 0.05, as tested by ANOVA, demonstrating the flexibility of selecting RGB reader application.

Table 3. Linear regression parameters of the standard curves from different color readout applications. ($n = 3$)

Applications	Slope ± S.D.	Y-intercept ± S.D.	R^2
Color grab (Android)	0.0114 ± 0.0002	0.0045 ± 0.0086	0.9992
RGB color picker (Android)	0.0114 ± 0.0003	0.0036 ± 0.0073	0.9995
Color name (iOS)	0.0114 ± 0.0002	0.0034 ± 0.0111	0.9996
Pixel picker (iOS)	0.0114 ± 0.0002	0.0033 ± 0.0071	0.9998

4.1.3.3 Type of smartphone

Because the quality of the smartphone camera has been continually improving, which directly impacts the quality and color of the image [128, 129], the different brands of smartphones were tested to validate inter-phone repeatability. The sample solutions were captured by an iPhone and two Android smartphones and interpreted to B value by the Color Name application. From the plotting of log B_0/B and drug concentration, the R^2 of linear regressions using images obtained from the iPhone 5s, Huawei nova 3i, and Samsung Galaxy Note 9 were 0.9996, 0.9731, and 0.9562, respectively. The result showed that two Android smartphone brands were not fit to log B_0/B properly. The best-fitting models of these smartphones were given in Table 4, which represents the relationship of B values to drug concentrations. Nonetheless, the final results from the testing of the 25 µg/mL penicillamine solution were not significantly different when computed using the regression equation that was the best model for each device. Accordingly, it should be noted that the assay presented in this work was developed and tested for an iPhone, and it is recommended that the appropriate regression model should be carefully selected for the calculation and/or perform color calibration [109, 130, 131] before using the method with other smartphones.

Table 4. The best-fitting models and the final concentrations of sample obtained from the assay using different smartphones brands.

Smartphone	Regression equation	R^2	Found concentration[a] (µg/mL)
iPhone 5s	$y = 0.0114x + 0.0034$	0.9996	24.62 ± 0.38
Huawei nova 3i	$y = 0.0214x^2 + 3.7955x - 5.1487$	1.0000	24.54 ± 0.54
Samsung Galaxy Note 9	$y = 0.0080x^2 + 4.2786x - 10.1480$	0.9992	24.80 ± 0.55

[a] Determined by using penicillamine solution of about 25 µg/mL ($n = 5$); for one-way ANOVA at 95% confidence level, the experimental F-value = 0.3500 and the critical value = 0.3885.

4.1.4 Analytical performance

Under the optimized conditions described above, the proposed assay demonstrated an excellent linear relationship between log B_0/B and penicillamine concentrations ranging from 5 to 40 g/mL, as evidenced by linear standard curve shown in Figure 18C, and the regression analysis results with a coefficient of determination (R^2) of 0.9996 (Table 5). From the regression equation, it was found that LOD and LOQ of method was low and sufficiently sensitive for the analysis of drug content in the formulations. The current method is accurate and precise by showing the % recovery values within 98–102% and % R.S.D. less than 2 for both repeatability and intermediate precision.

Table 5. Analytical characteristics of the smartphone-based assay of penicillamine

Characteristics	Results
Linearity	
Regression equation	log B_0/B = 0.0114C + 0.0034
R^2	0.9996
Range	5–40 µg/mL
LOD	0.99 µg/mL
LOQ	2.99 µg/mL
Accuracy (%recovery) ($n = 3$)	99.87 $\pm$ 0.45 (at 20 µg/mL penicillamine)
	99.74 $\pm$ 1.05 (at 25 µg/mL penicillamine)
	101.34 $\pm$ 0.10 (at 30 µg/mL penicillamine)
Precision (%R.S.D.)	
Repeatability ($n = 6$)	1.89
Intermediate precision ($n = 18$)	1.33

In terms of specificity, the approach was absent of interference from typical excipients used in capsule formulations, such as penicillamine disulfide, silicon dioxide, magnesium stearate, and lactose (Table 6). Because these contaminants lacked free thiol groups to react with Ellman's reagent, and because some of them

were almost insoluble in water, they were eliminated by filtering prior to the colorimetric reaction. The effect of the capsule shells, which were made of gelatin and colorants, on the interfering effect was also examined. Because of large dilutions, the capsule shells had low effect to the analysis.

Table 6. Specificity of smartphone-based assay of penicillamine. ($n = 3$)

Interference	Concentration added*	%Recovery
Lactose	40 %	101.36
Magnesium stearate	5 %	99.15
Sodium starch glycolate	8 %	99.94
Silicon dioxide	5 %	99.15
Penicillamine disulfide	4 %	99.46
Capsule shell	One shell / 250 mg penicillamine	101.09

* The concentrations were % weight by weight of interferences in the formulation, except for penicillamine disulfide in which the added concentration is expressed as % weight of penicillamine disulfide to weight of penicillamine.

4.1.5 Applications to the assay of real samples and comparison with reference methods

4.1.5.1 Quantitation of penicillamine for drug quality control

Table 7 showed the results of penicillamine capsule assay and dissolution test. The validated smartphone-based method was applied to the quality testing of the commercial penicillamine capsules compared with reference methods. The findings of the content assay obtained from the smartphone-based method, microplate reader method, and HPLC method were not statistically different with calculated and critical F-values of 0.0568 and 3.8853, respectively, according to the one-way ANOVA at 95 percent confidence level. To compare one by one, the estimated t-values for smartphone-microplate reader, smartphone-HPLC, and microplate reader-HPLC were –1.1171, 2.2284, and 1.4891, respectively, with a critical t-value of 2.5706, confirming that these procedures were not significantly different. It is noteworthy that the time required for the analysis using the smartphone-

based method was shorter, generally less than 15 minutes to analyze 6 standards and 6 samples. Because no chromatographic column equilibration was necessary, and numerous samples could be captured in a single shot. As a result, colorimetric measurement of penicillamine using a smartphone is a quick, simple, low-cost, and reliable assay.

In another viewpoint, the developed method can be adapted for use in a semi-quantitative dissolution test in the first stage (S1). From B value comparison, the values read from the samples were immediately compared with the value acquired from a reference solution containing a drug concentration at the acceptance criterion. In this investigation, B values obtained from six individual units were in the range of 123 to 131. They were less than the B value of 140 obtained from 23.6 µg/mL penicillamine standard solution (equivalent to Q + 5%). Due to the higher concentration, this will show a lower B value as described in section 4.1.1. So, it means that samples were released at a higher amount than standard criteria. Other than that, % drug releases of six samples were also calculated to confirm that every single capsule was released more than 85% (Q + 5%) in 30 min (Table 7), indicating that all capsules released the drug met the criteria. According to the results, smartphone-based methods is an excellent option for analyzing penicillamine formulations throughout the production process. It also showed a great chance of being used to the assessment of currently available thiol-containing drugs such as tiopronin, N-acetylcysteine, captopril, mesna, and others with drug contents ranging from 10 to 1,000 mg per unit. After the test has been improved and verified, the suggested approach might be used to quantify these drugs. However, it should be noted that, due to the lower sensitivity of the smartphone technique compared to spectrophotometry, the application of the smartphone-based Ellman's colorimetric method for low-dose drug formulations should be approached with caution.

Table 7. Results of penicillamine capsule assay and dissolution test

Analysis	% Labeled amount or % drug released			
	Smartphone	Microplate reader	HPLC	% relative error [d]
Assay of content [a, b]	96.14 ± 1.16	96.20 ± 0.56	96.31 ± 0.56	0.18
Dissolution test [c] (1st stage)	92.35, 95.35, 92.35, 94.34, 96.36, 100.51	92.94, 96.78, 93.08, 95.84, 95.40, 99.98	93.51, 96.80, 93.77, 95.59, 96.51, 99.82	0.15 – 1.52

[a] The acceptance criteria is 90–110 % labeled amount
[b] $n = 5$
[c] The acceptance criteria is > Q + 5 (85%).
[d] Calculated by |result$_{Smartphone}$ - result$_{HPLC}$|/result$_{HPLC}$ x 100

4.1.5.2 Quantitation of free sulfhydryl groups in thiolated polymer

Since pharmaceutical analysis investigates not only drugs, but also pharmaceutical excipients, the smartphone-based Ellman's assay was tested for its efficacy for evaluating excipients during the development and synthesis process. Thiol, in addition to being a functional group in various drugs, is known to interact with cysteine-rich mucin residues via the creation of disulfide bond linkages. Thus, adding thiol groups to polymers is a quick and easy way to make mucoadhesive polymers for drug delivery systems. In this study, cysteine-conjugated chitosan was used to study which was synthesized following a procedure described by Sahatsapan et al. [92]. The free sulfhydryl groups in the thiolated polymer were determined using cysteine standards as a standard curve, employing a smartphone-based approach and the spectrophotometric method using the microplate reader. As demonstrated in Table 8, the regression equations derived from them were linear, with an R^2 greater than 0.9990. Despite the fact that the smartphone method was less sensitive than the absorbance measurement, as seen by the greater LOQ and LOD, it was effective for the analysis. Furthermore, the signals gathered by the two approaches, log B_0/B and absorbance, were strongly correlated across the concentration range investigated (Figure 21). The cysteine-conjugated chitosan sample comprised 17.83 ± 0.39 and 18.05 ± 0.34 µmol free thiol groups per gram polymer as evaluated by the smartphone method and the

spectrophotometric method using the microplate reader, respectively ($n = 6$). At a 95% confidence level, there was no statistical difference between the averages of the two approaches since the experimental t-value (1.0427) was smaller than the critical t-value (2.2281). These findings revealed that the smartphone-based assay was promising for simultaneous analysis of several samples and may be utilized as an alternative to the expensive absorbance measurement by microplate reader.

Table 8. Comparison of analytical characteristics derived from the smartphone-based method and the spectrophotometric method using the microplate reader for the assay of sulfhydryl groups in thiolated polymer [a].

Characteristics	Smartphone	Microplate reader
Linearity		
Regression equation	$\log B_0/B = 0.0015C - 0.0062$	Absorbance $= 0.0058C - 0.0367$
R^2	0.9997	0.9999
Range (µM thiol groups)	30–230	30–230
LOD (µM)	4.98	2.55
LOQ (µM)	15.08	7.73

[a] Studied by using L-cysteine as a standard.
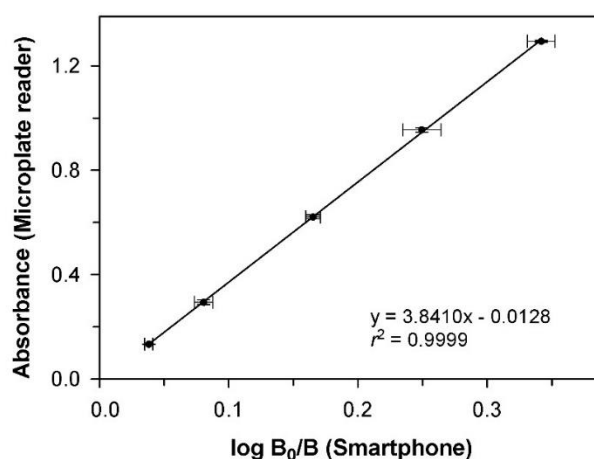
Figure 21. Correlation between the signals gathered by the smartphone-based method ($\log B_0/B$) and the spectrophotometric method (Absorbance) for the cysteine-conjugated chitosan assay.

4.2 DEVELOPMENT OF SMARTPHONE-BASED ION-PAIR EXTRACTION

4.2.1 General aspects

In this work, CPZ tablets was used as an example. Due to its colorless, sample was formed complex with dye to enable color expression. The formation of an ion pair in an acidic medium between the protonated amino group of the drug and the negatively charged sulfonate group of the MO dye was performed as shown in Figure 22. When the CPZ–MO combination was extracted using an organic solvent, it yielded a yellow-colored solution with a maximum absorbance of 415 nm. (Figure 23).
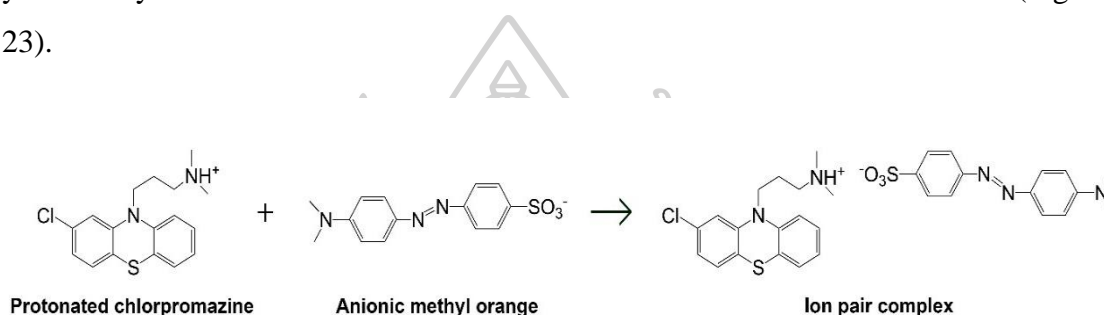
Figure 22. Formation of the ion-pair complex of CPZ and MO
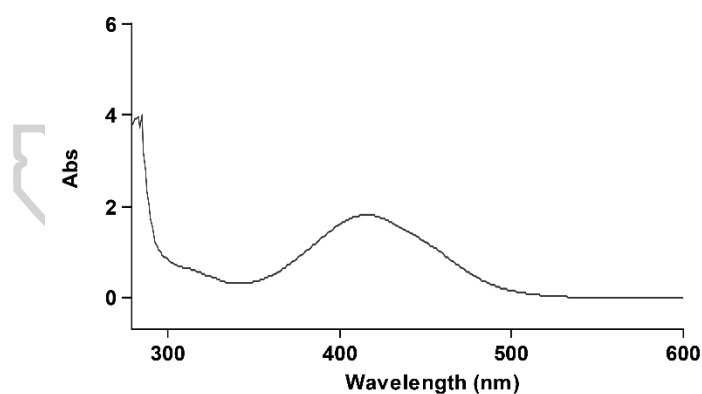
Figure 23. Absorption spectrum of the ion pair complex of CPZ and MO

4.2.2 Optimal conditions for ion pair extraction

4.2.2.1 pH of the reaction

Because pH influences CPZ and MO ionization, the optimal pH was determined using a variety of buffers, including HCl–KCl buffer (pH 1), potassium hydrogen phthalate buffer (pH 2–5), sodium citrate buffer (pH 6), and sodium phosphate buffer (pH 7–8). Other parameters were fixed using 0.2

mg/mL of MO and 800 µL of ethyl acetate for the study. Notably, the absorbance of the extract increased while pH was decreased from 8 to 2 (Figure 24A). Because chlorpromazine base, which has a pK_a of 9.3, was more protonated under acidic conditions, resulting in more positively charged CPZ molecules. It could form an appropriate complex with the negative charge of MO. However, at pH 1, the absorbance obviously decreased because MO, which is an acidic dye with a pK_a of 2, is in neutral form. As a result, the complex was rarely created. This conclusion supports previous research that demonstrated MO to be an effective ion pair reagent at low pH [35, 103, 104]. The standard curve in Figure 24B, derived from the extraction at pH 2, exhibited the greatest slope, showing the highest sensitivity. Based on these findings, pH 2, which was regulated with a potassium hydrogen phthalate buffer, was chosen as the optimal pH for the proposed technique.
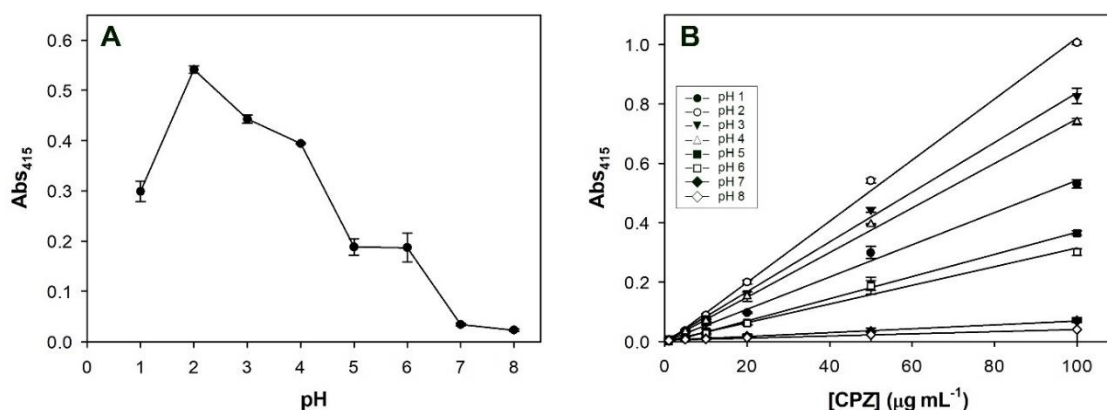
Figure 24. Plot of absorbance versus pH when 50 µg/mL of CPZ was extracted (A) and the standard curves for each pH (B).

4.2.2.2 Concentration of MO

The experiments were conducted using MO in the concentration range of 0.2–1.8 mg/mL extracting with 800 µL of ethyl acetate at pH 2. The results revealed that the absorbance continuously increased and reached a plateau at 1 mg/mL MO (Figure 25A). Despite the fact that the CPZ–MO stoichiometry was proven to be 1:1 (Figure 26), the introduction of excess MO resulted in successful extraction, most likely by supporting in reaching the equilibrium of ion pair formation and stabilizing the complex produced [102]. As a result, a 1

mg/mL MO solution was selected since it produced a high-sloped standard curve (Figure 25B) while saving reagent.
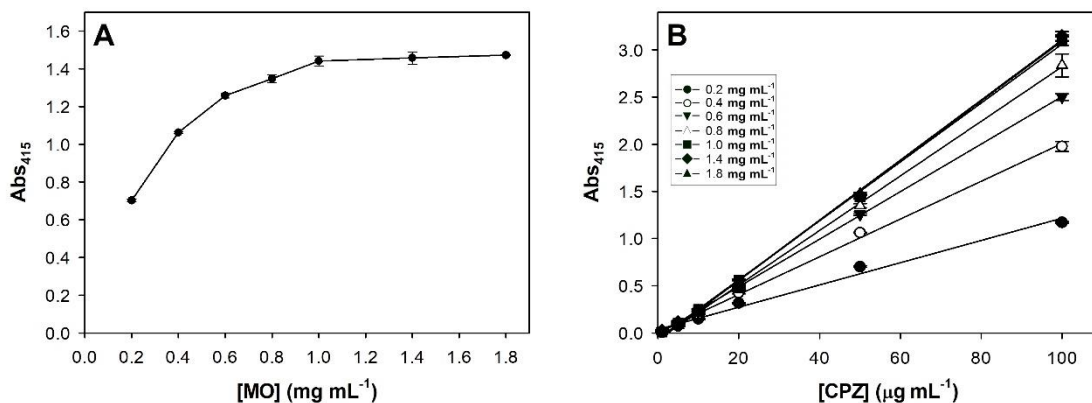
Figure 25. Plot of absorbance versus MO concentration when 50 µg/mL of CPZ was extracted (A) and the standard curves for each concentration (B).
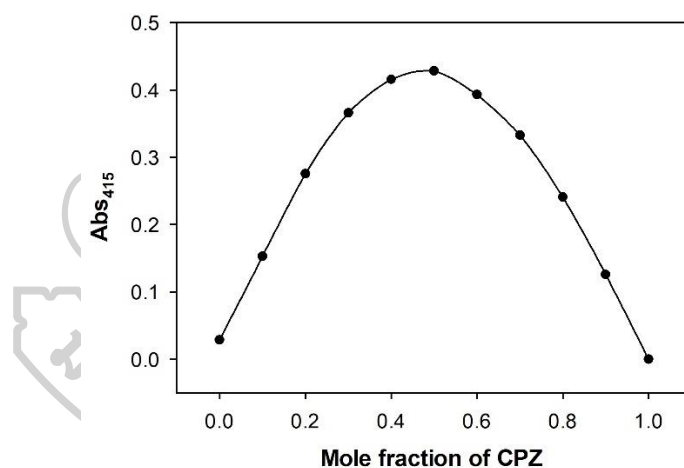
Figure 26. CPZ–MO stoichiometry.

4.2.2.3 Type of organic solvent

Green solvents including ethyl acetate, *n*-butyl acetate, and *n*-amyl acetate [132, 133], as well as chlorinated solvents including diethyl ether, dichloromethane, and chloroform, which is used in the USP method, were evaluated for use as extractants. The experiments were conducted at pH 2 using 1 mg/mL MO. As shown in Figure 27, chloroform produced the standard curve with the highest absorbance value and slope, indicating the greatest extraction capacity. Meanwhile, ethyl acetate and dichloromethane gave similarly standard curves, but a bit lower than chloroform. However,

chloroform and dichloromethane have been identified as carcinogens and potential ozone depleting agents [134, 135]. Therefore, ethyl acetate was chosen because it gave an acceptable performance, and it is also a green extraction solvent since it is one of the least environmentally hazardous organic solvents and can be generated through agricultural processing [133].
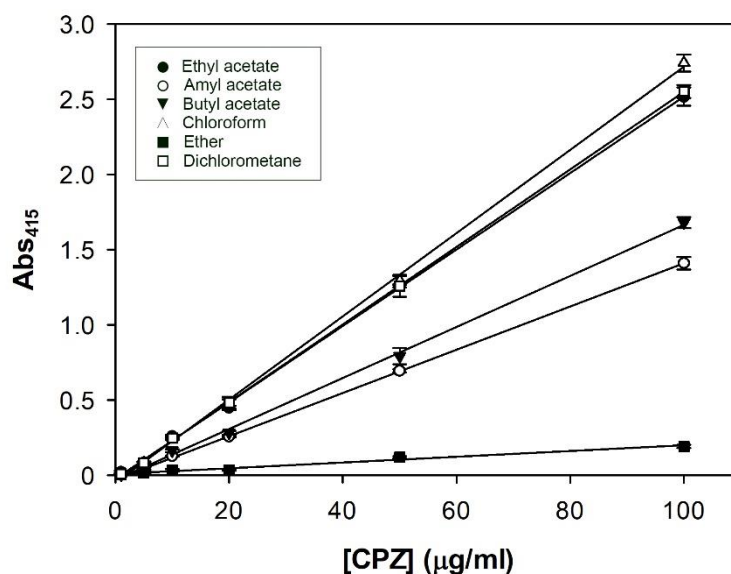
Figure 27. Standard curves for each type of organic solvent.

4.2.2.4 Extraction time

At the mixing point, the effect of vortex time was examined in the range of 30–240 s. The analysis was conducting at pH 2 using 1 mg/mL MO. Figure 28 showed the absorbance values of the ethyl acetate phase increased when the extraction time was increased up to 180 s and then remained constant at longer mixing times. Thus, 180 s or 3 min was used as an optimal time for extraction.
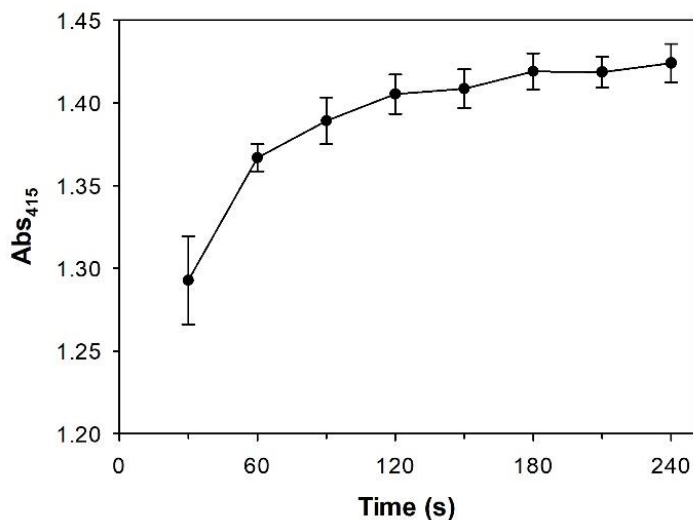
Figure 28. Plot of absorbance at 415 nm versus extraction time.

4.2.2.5 Volume of organic solvent

The impact of ethyl acetate volume was studied by doing the extraction with 500–800 µL of ethyl acetate. The experiments were conducted at pH 2 using 1 mg/mL MO. The amounts of extracted drug were arbitrarily calculated by multiplying the absorbance values of the extract with the volume used. As shown in Figure 29, the extraction efficiency was increased when a large volume of solvent was used, as shown by the large amounts of drug found in the extracts. Although 900 µL ethyl acetate could be added to 600 µL of the aqueous phase to achieve the maximum capacity of a 1.5 mL microcentrifuge tube, this was not suggested since there remained inadequate space in the tube for efficient mixing. So, 800 µL ethyl acetate was utilized as an optimal volume.
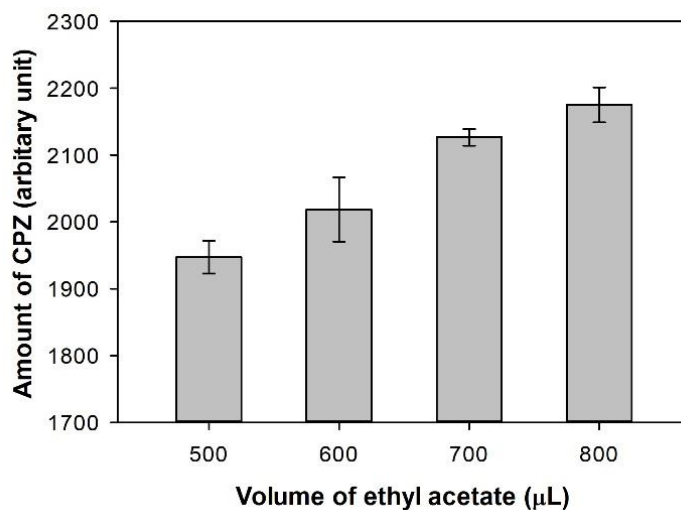
Figure 29. Amount of CPZ which was extracted with different volume of ethyl acetate.

Under the obtained optimal conditions, the extraction efficiency was tested for one-round extraction to ascertain its performance, which was the gold of this study. By extracting the same solution at 50 µg/mL for four times repreatly, the fraction of drug distributed into the first, second, third, and fourth round extracts were 92.2%, 7.2%, 0.5%, and 0.1%, respectively. This result indicated that a one-round extraction was sufficient for the assay since an extraction efficiency of more than 90% was produced. In prior research, single extraction was also employed [105, 107].

4.2.3 Selection of an appropriate RGB channel and data transformation

Following the optimal extraction procedure, standard solutions of 2.5–50 µg/mL were extracted to investigate the best corresponding color value to drug concentration. Figure 30A demonstrated that the basic B values, which represent the intensity of the blue color, a complementary color of yellow in the RGB model, were inversely related to drug concentration, with an R^2 of 0.9985, but the R and G values didn't vary with drug concentration. For this reason, the B value was chosen to be used for the assay. The appropriate mathematical transformations were reported, such as log B, B/255, or $\sqrt{R^2 + G^2 + B^2}$ [136], to give a better correlation. In this study, the B values normalized with the total of the RGB values as

$(\frac{B}{R+G+B})_{\text{blank}} - (\frac{B}{R+G+B})_{\text{CPZ}}$ showed the best correlation response and produced a standard curve that was more linear than the untreated B value, with an R^2 of 0.9998 (Figure 30B).
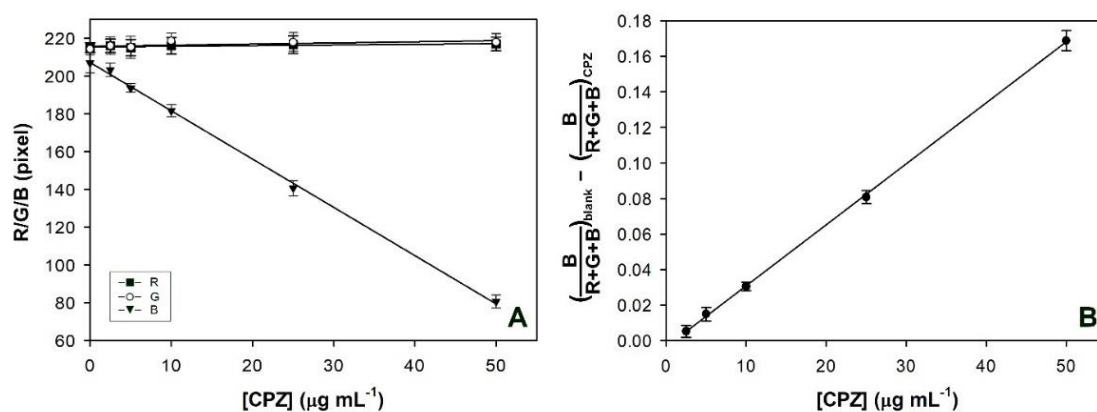
Figure 30. Plots of the untreated R, G, and B values versus the concentration of CPZ
(A) and the standard curve plotted using the normalized B values (B).

4.2.4 Optimal procedure for image acquisition

4.2.4.1 Tubes arrangement

The image capturing step was carefully carried out in order to establish an assay procedure that was reliable and reproducible. A set of tubes consisting of the standard tubes and sample tubes were designed to be captured at one time to allow for a shorter analysis time and less variation between shots. For this purpose, racks produced by the 3D printing technique were fabricated to hold multiple tubes in fixed, consistent positions throughout the image capture process. In addition, due to the unconsistency of the obtained image brightness, which was dimmer radially at the border, as reported above in section 4.1.3.1 (Figure 20), the appropriate arrangement of the tubes was investigated. By placing the tubes containing the same yellow-colored extract in a radial alignment (Figure 31A), the %R.S.D. for the B values (1.95%, $n = 18$) was significantly less than that determined from the tubes arranged in linear direction (Figure 31B) (6.64%, $n = 18$). Because of the equal distances from the central focusing point to the tubes, RGB values were affected equally among the tubes arranged in a radial direction. Furthermore,

the results obtained from the previously described B/(R+G+B) values showed less variation than the unnormalized B values, with an %R.S.D. of 1.51% and 2.18% for radial and linear tube alignment, respectively. Based on these findings, we can conclude that arranging the tubes in radial alignment during image capture, as well as using normalized B/(R+G+B) values, can limit the variation of the analytical signals caused by brightness shading.
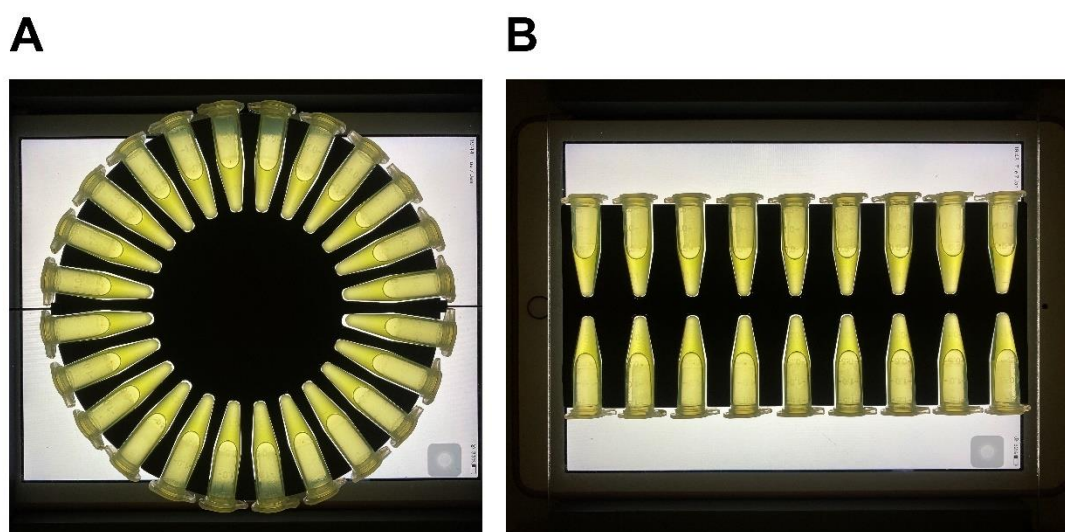
Figure 31. The arrangement of tubes in a radial alignment (A) and linear alignment (B).

4.2.4.2 Luminous intensity of light source

In this work, a tube holding a yellow-colored extract was captured when the screen of the iPad, which acted as a light source, was adjusted to different brightness levels. Figure 32A showed the image of CPZ extraction obtained when captured at difference brightness. The results showed that when the brightness of light increased, the B values were changed to be higher value (Figure 32B), whereas the B/(R+G+B) values were not affected (Figure 32C). As a result, it was appropriate to use normalized B/(R+G+B) values.
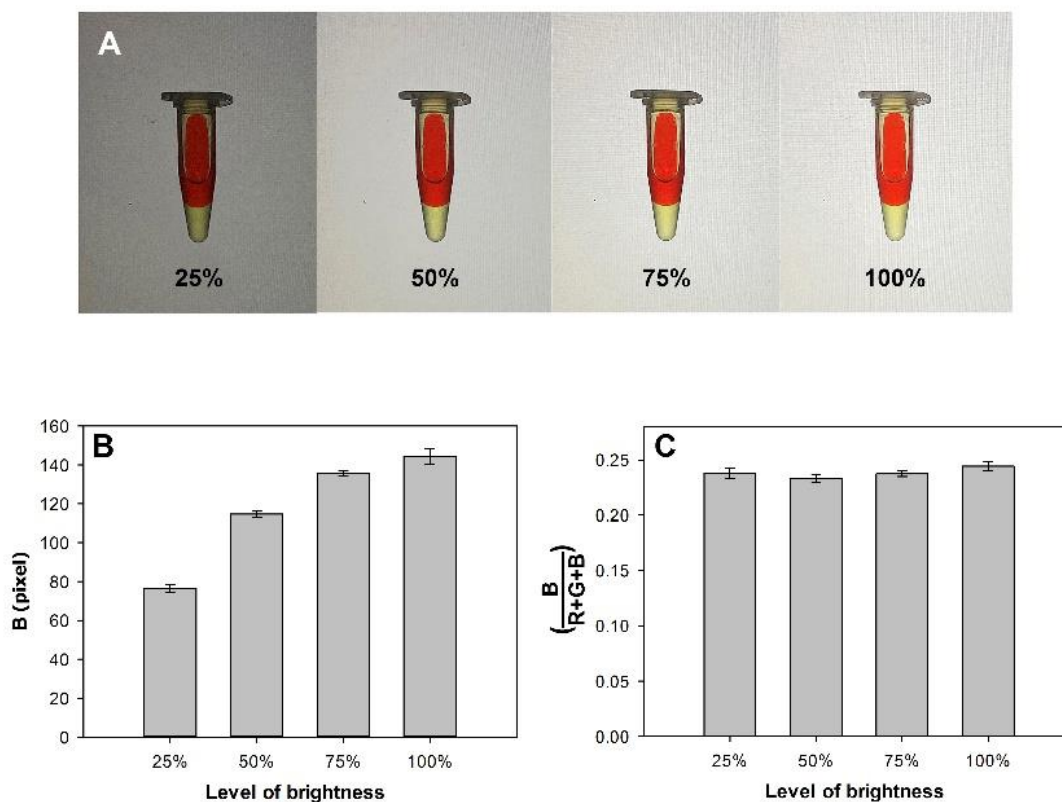
Figure 32. Images captured using the screen of the iPad as light source set at different brightness levels (A) and effects of the brightness of the screen on the B values (B) and normalized B values (C).

4.2.4.3 Tube turbidity

To determine if the presented procedure is suitable for laboratories with varying types of equipment, clear-wall and turbid-wall microcentrifuge tubes from various manufacturers were examined. The results showed that the turbid-wall tubes gave a standard curve with slightly lower slopes. Whereas the %LA of six samples calculated from their own calibration curve were not statistically different in two types of tubes with a 95% confidence interval (pair *t*-test = 0.7184, critical *t*-test = 2.7764). However, the use of tubes with high transparency is recommended to ensure high sensitivity of the assay.

4.2.5 Analytical performance

Table 9 summarizes the validation findings. The proposed method showed good linearity in the concentration range of 2.5–50 µg/mL CPZ. The LOD and LOQ indicated the sufficient sensitivity of the method for the quality control tasks in the

pharmaceutical industry because CPZ tablets are available as 10–200 mg doses. The method was accurate and precise, with the %recovery in the acceptable range of 98% to 102% at all three concentration levels tested. In addition, the %R.S.D. values of the assay results obtained from both interday, and intraday precision studies were <2%, proving that the method was precise.

Table 9. Validation results of the method

Parameters	Results
Regression equation	Y = 0.0034 X – 0.0034
	when $Y = (\dfrac{B}{R+G+B})_{blank} - (\dfrac{B}{R+G+B})_{CPZ}$ and
	X is concentration of CPZ (µg/mL)
R^2	0.9998
Range	2.5–50 µg/mL
LOD	0.76 µg/mL
LOQ	2.30 µg/mL
Accuracy (%recovery, $n = 3$)	
	100.46 ±0.77 % (20 µg/mL)
	99.55 ±1.07 % (25 µg/mL)
	99.32 ±0.72 % (30 µg/mL)
Precision (%R.S.D.)	
Interday precision ($n = 18$)	1.53
Intraday precision ($n = 6$)	1.09

In the study of specificity, CPZ was assayed in the presence of three common excipients. The results showed that the obtained %recovery of lactose, magnesium stearate, and silicon dioxide were 100.18%, 98.10%, and 98.95%, respectively. This result indicated that the excipients unaffected to the assay because of the lack of a functional group that could be ionized and then form an ion-pair complex with MO. Furthermore, because some of these compounds are insoluble in water, they have been removed by filtering during the preparation.

4.2.6 Application to the assay of real samples and comparison with reference methods

Commercial CPZ tablets were studied to compare the results obtained from the proposed method and the reference method. The average of %LA ($n = 6$) resulting from the smartphone-based method and the USP43 method were 99.28 ± 1.64% and 99.46 ± 1.27%, respectively. It showed no significant difference between the two methods with a 95% confidence interval, testing by Student's t-tests. As a result, smartphone-based ion-pair extraction was a good alternative due to ease of use, less time required, and low cost. Moreover, there was less reagent consumed and the use of less harmful solvents, resulting in a lower generation of waste and a reduction of chemical exposure according to the green chemistry principle.

4.3 DEVELOPMENT OF SMARTPHONE-BASED TITRATION RELYING ON VOLHARD'S METHOD

4.3.1 Selection of an appropriate RGB channel and data transformation

To find an equivalence point from a linear-segment curve, the intersection of two straight lines representing the before and after equivalence point regions was calculated. In the titration process, the miniaturized titration published by Rojanarata et al. [18] was adapted using a smartphone-based method. The solution color was colorless throughout the first time, and the intensities of all color values were rather stable. After reaching the equivalence point, the orange color appeared, and higher intensity was seen, which was related to G and B values decreasing while R values slightly increasing in a non-linear response. (Figure 33A). Although B values were more sensitive than G values because they decreased more quickly, the values hit zero when 140 µL of ammonium thiocyanate solution was added to the titration, restricting the use of larger volumes of titrant. For this reason, the G value was chosen to be used to monitor color change in the titration.
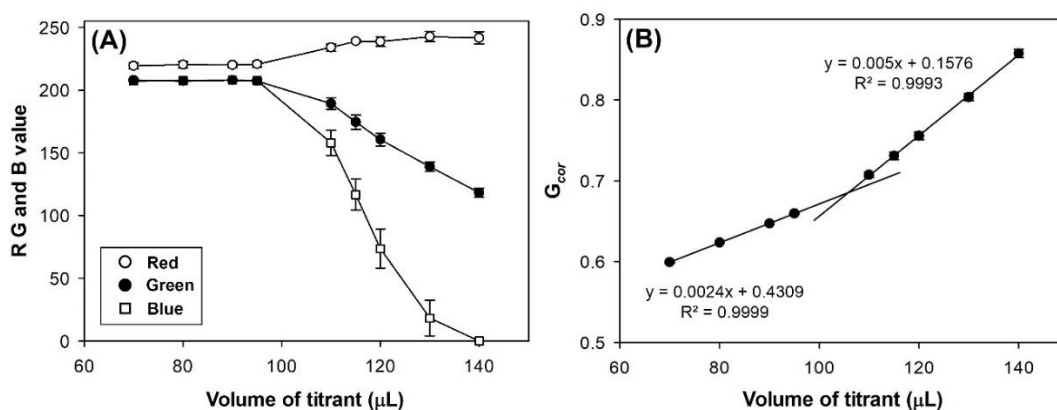
Figure 33. Plot of volume of titrant (NH$_4$SCN) versus RGB values (A) and G$_{cor}$ (B).

The previous reports showed variety of mathematical models used for the transformation of RGB values to create the best signal response, such as 255–B [137], (G−G$_{blank}$)/255 [35], G/R ratio [54], and log(P/P$_o$) [60, 138]. Consequently, the transformation of G values was explored further using various mathematical models, and the results were proven in terms of improved linearity of the lines on the titration curve. As shown in Table 10 and Figure 33B, a 1/log G, which was then corrected for the impact of volume change owing to titrant addition, generated two lines with a strong linear relationship to the volume of titrant added (R^2 > 0.9990) in the sections before and after the equivalence point. As a result, corrected 1/log G (G$_{cor}$), which was calculated following Equation 1, was utilized to create a linear-segment curve for the titration.

$$G_{cor} = \frac{1}{\log G} \times \frac{V_0 + V}{V_0} \text{ --- (Equation 1)}$$

where V$_0$ is the initial volume of supernatant in a tube, and V is the volume of 0.01 M NH$_4$SCN added.

Table 10. R^2 of the titration curve in two regions obtained from different mathematical transformations of RGB values ($n = 3$).

Analytical signal	R^2 of the relationship between the signal and volume of titrant	
	Before equivalence point	After equivalence point
G	0.9983	0.9961
G_{s-b}*	0.0004	0.9979
log G	0.9999	0.7520
1/log G	0.9999	0.9993
G/(R+G+B)	0.9985	0.7602
$\sqrt{R_{s-b}^2 + G_{s-b}^2 + B_{s-b}^2}$ *	0.9584	0.9657

* R_{s-b}, G_{s-b}, and B_{s-b} are the RGB of sample corrected for the blank.

To demonstrate the range in which G_{cor} responded linearly to the volume of titrant added, the titration was conducted by adding the titrant in the ranging from 20 µL to 240 µL and the color intensities of the resulting solutions were then measured by using smartphone. The results from the smartphone-based method were also compared to those obtained from the absorbance measurement method using a microplate reader. When the titrant volume was raised to 240 µL, a plot of G_{cor} versus titrant volume was linear in the post-equivalence point area, with an R^2 of 0.9990 (Figure 34A). The plot utilizing absorbance values, on the other hand, curved at a large volume of titrant applied (Figure 34B) due to absorbance variations that occurred at a high concentration of analyte, in accordance with Beer–Lambert's law [139]. In the case of the absorbance measurement method, if the titrant volume was used in the range of 110–140 µL, the R^2 of the post-equivalence point area was 0.9991, while if a higher titrant volume, such as 180 µL, was used, the R^2 of the post-equivalence point area was decreased to 0.9953. Although diluting samples prior to absorbance testing can solve this problem, it offers extra steps and increases the probability of sample loss.
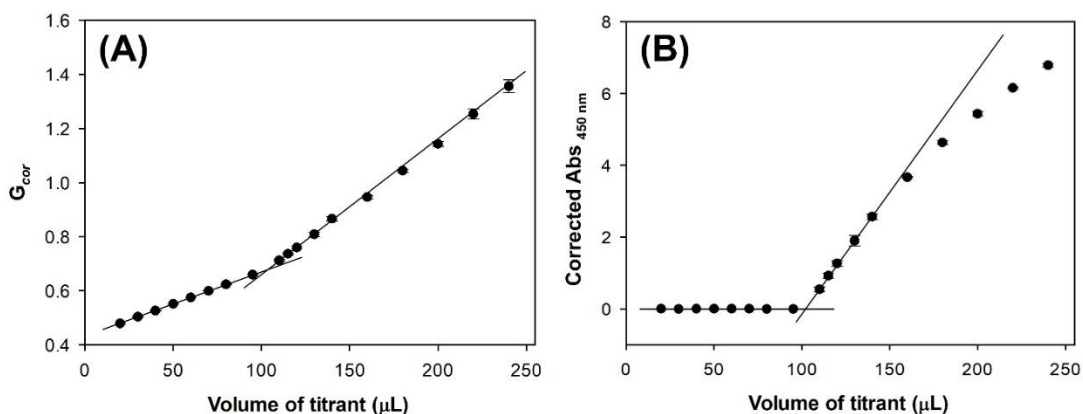
Figure 34. Plot of volume of titrant (NH$_4$SCN) versus G$_{cor}$ (A) and absorbance at 450 nm (B) when the volume of titrant (NH$_4$SCN) in the range of 20–240 µL was studied.

To compare the obtained equivalent point from two methods, the same number of data (4 points before and 5 points after the equivalence point) was used for the determination of intersection point. The average of equivalence points ($n = 6$) obtained from the smartphone-based method and absorbance methods were 104.43 ± 0.32 and 103.70 ± 0.97, respectively. The statistical results showed no significant difference between the two methods, with 95% confidence interval (t-value = 1.7499 and critical t-value = 2.2281). Therefore, using corrected G values derived from the proposed study was not only useful in some locations where high-cost microplate readers are scarce, but it also provided an effective and simple method to perform a titration curve with a wider range of linearity.

4.3.2 Optimal procedure for image acquisition and color interpretation

4.3.2.1 Color of microplate wall

In general, microplates are often available in a variety of colors that are appropriate for a variety of applications. Clear (colorless) microplates are ideal for measuring absorbance in the visible range, such as in a colorimetric experiment. those with black walls are preferred for measuring fluorescence intensity because they reduce background, auto-fluorescence, and well-to-well crosstalk. In many smartphone-based colorimetric experiments, microplates are also utilized as containers while photographing samples [140]. However, the effect of their color on signal acquisition has not been studied. Therefore, this issue was investigated. The titration solution in clear-wall and black-wall

microplates was from the same batch of microtitration and was captured by the same smartphone.

As shown in Figure 35A, a black microplate gave higher G values than a clear microplate at every titration point. But, after G values were transformed and corrected following Equation 1 as described above (Figure 35B), the average of equivalence points ($n = 6$) obtained from clear-wall and black-wall microplate were 101.27 ± 1.92 and 100.98 ± 2.28, respectively. The statistical results showed no significant difference between the two types of microplates with a 95% confidence level (t-value = 0.8134, critical t-value = 2.5706). Similarly, when using the absorbance measurement method, the equivalence points were not different, with a 95% confidence level (t-value = 0.0215, critical t-value = 2.5706). These findings demonstrated that the color of microplate did not affect the sodium chloride assay by smartphone-based method when the color values were properly transformed and corrected. However, clear microplate was chosen to use in this study because it is cheaper than black ones.
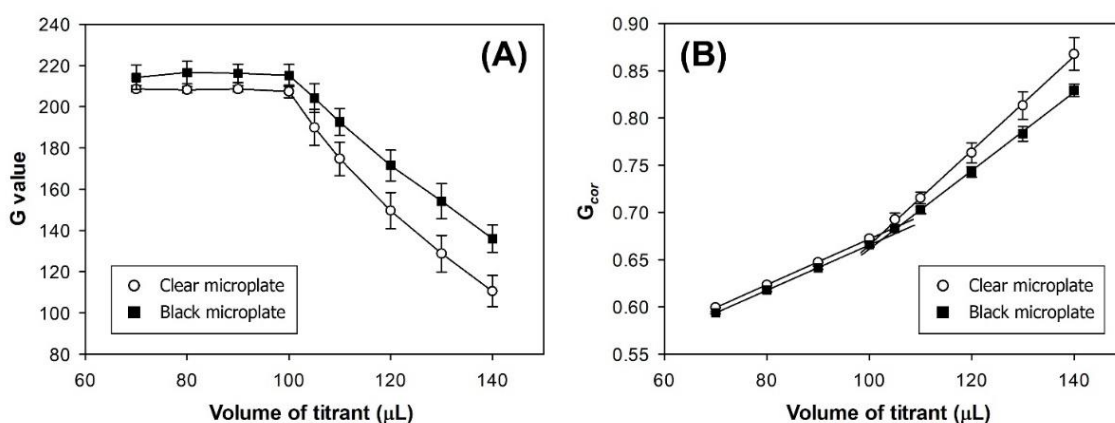
Figure 35. Plot of volume of titrant (NH$_4$SCN) versus G value (A) and G$_{cor}$ (B) when different microplate colors (clear wall and black wall) were used.

4.3.2.2 Type of light source

The %LA of samples ($n = 6$) determined from the smartphone-based method by using a tablet and LED lamps as light sources were 101.73 ± 0.21 and 101.84 ± 0.18, respectively. The use of a tablet screen was not

significantly different from the use of an LED lamp, with a 95% confidence level (t-value = −0.9557, the critical t-value = 2.2281). As a result, depending on device availability, either approach can be utilized to set up the light source in the study.

4.3.2.3 Type of smartphone

Three smartphones, including the iPhone 11 (iOS), Samsung Galaxy S20+ (Android), and Oppo Reno 3i (Android), containing a back camera with a resolution of 64, 64, and 12 megapixels, respectively, were used to capture the same result solutions in the same environment, and the obtained %LA from each device was then compared. Figure 36 shows that the image from iPhone 11 was brighter than the others, resulting in different G values being obtained. The calculated %LA of the iPhone 11, Samsung Galaxy S20+, and Oppo Reno 3i were 100.71 ± 0.29, 100.63 ± 0.16, and 100.52 ± 0.19, respectively. However, a one-way ANOVA demonstrated that these results were not significantly different, with a 95% confidence level (F-value = 1.1683, critical F-value = 3.6823). From the previous studies on smartphone-based colorimetric assays, the different smartphones might have produced different image properties, including RGB pixels. However, no difference was seen among the devices when the assay results were computed using their own data set, such as the RGB values of the standard and sample solutions, which were determined from an image in which they were taken simultaneously in the same picture [141].
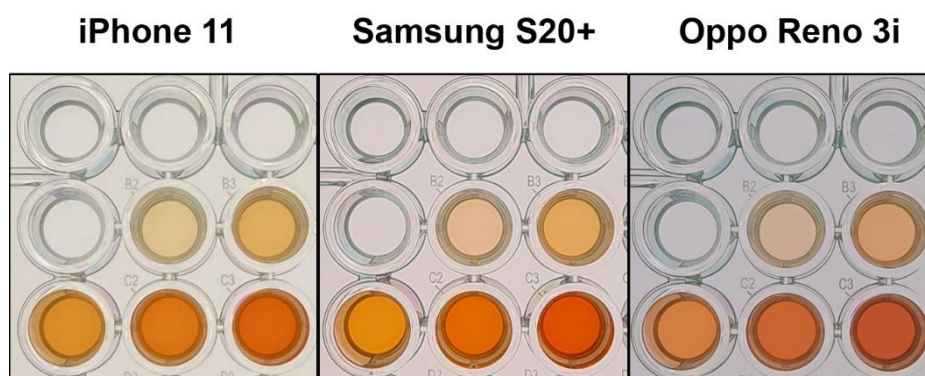
Figure 36. Effect of smartphone on the images captured from the same nine wells.

4.3.2.4 RGB analysis tool

In comparison with the analysis performed using different color detectors, ImageJ (ImageJ 1.53e, National Institute of Health, USA), a common freeware program for image analysis [76, 142-145], was used to analyze the color intensity in comparison with the Color Detector application on the smartphone. For ImageJ platforms, the images have to be transferred to a PC or notebook after being captured by the smartphone. Then the Color Histogram plugin was used to interpret the RGB values. The findings revealed that two platforms, which were ImageJ and the mobile application, produced almost comparable G values (Figure 37), showing that both can be utilized satisfactorily. However, in order to analyze RGB using ImageJ, the image has to be transferred from the smartphone to the PC. So, the mobile application was employed in this study since it is a practical way to RGB reading and then data analysis.
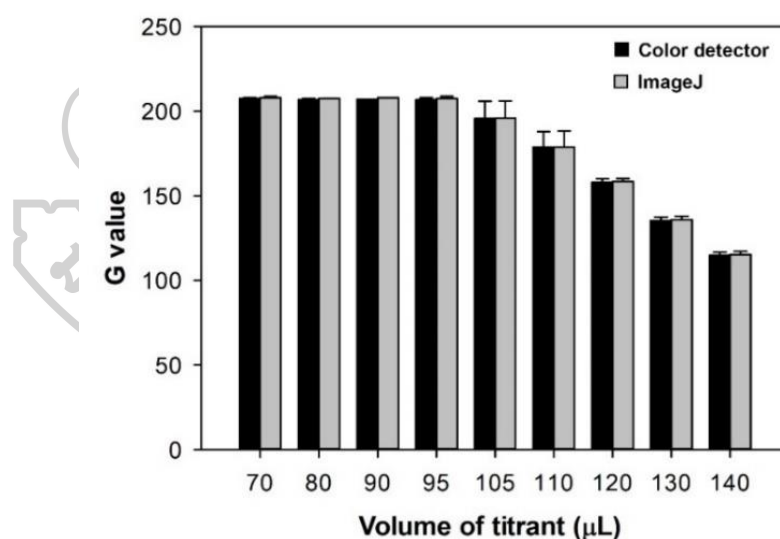
Figure 37. Plot of volume of titrant (NH$_4$SCN) versus G value read out by ImageJ and Color Detector mobile application.

4.3.3 Analytical performance

Table 11. Accuracy and precision results.

Parameter	Concentration of sodium chloride tested (% w/v)	Results*
0.45% w/v sodium chloride		
Accuracy ($n = 3$)	0.428	100.33 ± 1.18 %
	0.450	100.30 ± 1.28 %
	0.473	100.52 ± 1.01 %
Precision		
Intraday ($n = 6$)	0.450	1.18 %
Interday ($n = 18$)	0.450	1.04 %
Inter-analyst (3 analysts)	0.450	1.20 %
0.90% w/v sodium chloride		
Accuracy ($n = 3$)	0.855	100.17 ± 0.10 %
	0.900	100.30 ± 0.18 %
	0.945	98.92 ± 0.20 %
Precision		
Intraday ($n = 6$)	0.900	0.19 %
Interday ($n = 18$)	0.900	0.20 %
Inter-analyst (3 analysts)	0.900	0.46 %

* Accuracy results are reported as %recovery (average ± S.D.) and precision results are reported as %R.S.D.

After the optimal condition was obtained, the assay was validated. The equivalence points derived from the smartphone-based method showed a good linear correlation (R^2 of 0.9998) to the NaCl concentration in the range of 0.4163–0.9675 %w/v (Figure 37). The proposed method was accurate, as indicated by %recovery in the range of 98%–102%, when the three concentration levels of 0.45% and 0.90% w/v NaCl were analyzed (Table 11). Furthermore, the %R.S.D. values of the interday, intraday, and inter-analyst precision studies were less than 2%, indicating that the method was precise.
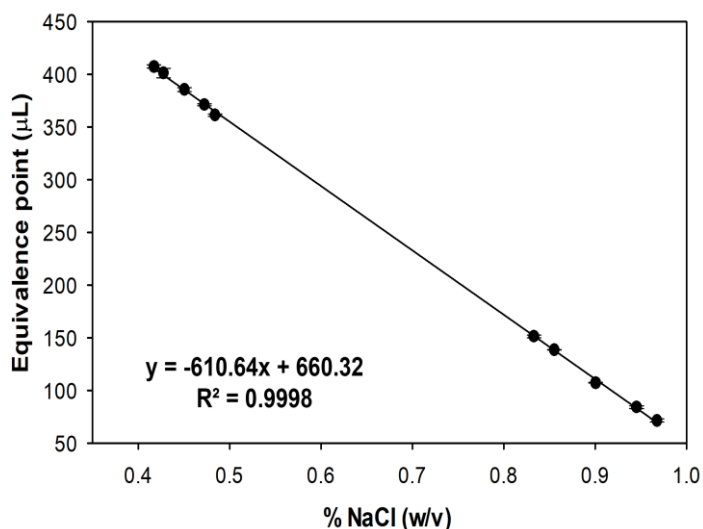
Figure 38. Plot of NaCl concentration versus equivalence point acquired from the smartphone-based method.

4.3.4 Application to the assay of real samples and comparison with reference methods

The proposed smartphone-based microtitration was studied to compare the obtained results with the spectrophotometric and USP43 methods by using the commercial 0.45% and 0.90% w/v sodium chloride injections from three different manufacturers as a sample. As shown in Table 12, all methods gave %LA of sodium chloride injection samples that were within the USP acceptance criteria of 95.0–105.0%. Importantly, the paired *t*-tests indicated no significant difference between the results obtained from the smartphone method versus USP43 method and the smartphone versus microplate reader method. These findings indicated that the smartphone-based method, which relies on the intersection of an RGB linear-segment curve to determine an equivalent point, was effective in the microtitrimetric assay of sodium chloride injections. Furthermore, it can be used to determine sodium chloride in raw materials and tablets, as shown by previous studies [18], in which its protocol had a similar principle to that followed in this work.

Table 12. Sodium chloride assay in three commercial brands

Sample	Method	% labeled amount						Paired *t*-value*	
		Brand 1-1	Brand 1-2	Brand 2-1	Brand 2-2	Brand 3-1	Brand 3-2	Smartphone vs USP43	Smartphone vs microplate reader
0.45% w/v NaCl injection	Smartphone	100.71	100.60	100.49	100.60	100.19	99.91	-1.4767	-1.4775
	USP43	100.67	100.67	100.60	100.60	100.67	99.99		
	Microplate reader	101.16	101.02	100.61	100.85	100.09	99.74		
0.90% w/v NaCl injection	Smartphone	100.69	100.65	100.74	100.32	100.77	100.64	-0.2838	0.9295
	USP43	100.62	100.62	100.62	100.62	100.75	100.69		
	Microplate reader	100.83	100.29	100.33	100.74	100.50	100.37		

* Critical *t*-value = 2.5706, *p*-value > 0.05

CHAPTER 5
CONCLUSIONS

This research demonstrates the applicability of smartphones for pharmaceutical analysis performed by the measurement of RGB values. Three analytical methods for drugs and excipient were developed and studied. In the first work, D-penicillamine was analyzed by using Ellman's assay. The image of the resulting reaction in a microplate was captured in a dark box over the array which did not exceed 7x7 wells to reduce the uneven brightness of different positions on the image. The investigation of the suitable RGB values which correlated to the yellow color of the reaction revealed that the transformed B value in term of $\log B_0/B$ showed a good linear relationship to the drug concentration. Although different smartphone brands might give different linear regression models, the issue did not affect the analytical results if the samples and standards were photographed in the same shot using the same smartphone and compared to each other using their own regression equation. In this work, the developed method was also successfully applied to the analysis of thiol groups in cysteine conjugated chitosan. It was confirmed that there was no significant difference between the results obtained from using a smartphone and that from a microplate reader.

In the second work, small-scale extraction for the assay of chlorpromazine hydrochloride was investigated. Methyl orange dye was used to form an ion-pair complex under the optimal conditions with the analyte and the complex was extracted into ethyl acetate, showing yellow color. The tubes of standards and samples were arranged in a radial 3D-printed rack in the light-controlled box and photographed in the same shot without a transfer of organic phase. The $(\frac{B}{R+G+B})_{\text{blank}} - (\frac{B}{R+G+B})_{\text{CPZ}}$ value gave the best-fitted curve with drug concentrations. The method was accurate, precise, unaffected by excipients, and sensitive enough for the assay of the drug in formulation. The results obtained from the smartphone-based method were not significantly different from that determined by the USP method as well as the method using a microplate reader. The benefits of the research over the previous reports were

the operation without phase separation and the image capture platform in the radial alignment which was capable of analyzing multiple samples. Because of that, the variations between tubes and between shots were low, and the method resulted in a fast analysis and low risk of exposure to hazardous organic solvent.

In the last work, smartphone-based colorimetry was developed for the titrimetric assay of sodium chloride relying on Volhard's method. This was the first time representing the correlation of titrant volumes and signals in a linear segment curve using RGB values. Chloride ions reacted with excess silver nitrate in the tube. Then, the solution containing residual silver ions was aliquoted in the equal volumes into the tubes. They were titrated back with ammonium thiocyanate by using ferric alum as an indicator and centrifuged to remove silver thiocyanate precipitate. The supernatants of each tube were transferred into the microplate then the image was captured in the light-controlled box. The reddish orange color related to the corrected $1/\log G$, which gave a good relationship with volumes of titrant added. The equivalent point could be calculated from the intersection of the two straight lines located in the regions before and after the equivalence point. The developed method showed comparable results with the USP method and the absorbance measurement using a microplate reader. It was accurate, precise, and sufficiently sensitive for the assay and quality control of sodium chloride injections. The proposed method was not affected by the color of the microplate wall, smartphone devices, or RGB reader applications. Moreover, the use of a linear segment curve could enhance the reliability of the titration by avoiding human judgment error from endpoint reading, which is a drawback of traditional titration.

To summarize this work, smartphone-based colorimetry was found to be not only reliable, but also simple, fast and inexpensive. Moreover, it could enhance the safety and environmental friendliness of the certain methods. Therefore, smartphone-based colorimetry has high potential to be used for alternative pharmaceutical analysis.

REFERENCES

1.   Errayess SA, Idrissi L, Amine A. Smartphone-based colorimetric determination of sulfadiazine and sulfasalazine in pharmaceutical and veterinary formulations. Instrumentation Science & Technology. 2018;46(6):656-75.

2.   Ping J, He Z, Liu J, Xie X. Smartphone-based colorimetric chiral recognition of ibuprofen using aptamers-capped gold nanoparticles. Electrophoresis. 2018;39(3):486-95.

3.   Hosseinimehr SJ, Ebrahimi P, Hassani N, Mirzabeigi P, Amini M. Spectrophotometric determination of captopril with DTNB reagent in pharmaceutical formulation. Bollettino Chimico Farmaceutico. 2004;143(6):249-51.

4.   Beales D, Finch R, McLean AE, Smith M, Wilson ID. Determination of penicillamine and other thiols by combined high-performance liquid chromatography and post-column reaction with Ellman's reagent: application to human urine. Journal of Chromatography B: Biomedical Sciences and Applications. 1981;226(2):498-503.

5.   Elbashir AA, Awad SF. A new spectrophotometric method for determination of penicillamine in pharmaceutical formulation using 1, 2-naphthoquine-4-sulfonate (NQS). Journal of Pharmacovigilance. 2013;1(2):1000105.

6.   Elbashir A, Alfadil A. Development and validation of spectrophotometric method for determination of penicillamine (pa) in pharmaceutical formulation using 4-choro-nitrobenzo-2-oxa-1, 3-diazol (NBD-CL). Journal of Analytical Chemistry. 2013;1:18-22.

7.   Naik RM, Prasad S, Kumar B, Chand V. Kinetic assay of D-Penicillamine in pure and pharmaceutical formulations based on ligand substitution reaction. Microchemical Journal. 2013;111:97-102.

8.   Mahajan PG, Kolekar GB, Patil SR. Recognition of D-Penicillamine Using Schiff Base Centered Fluorescent Organic Nanoparticles and Application to Medicine Analysis. Journal of Fluorescence. 2017;27(3):829-39.

9.   Pawar SP, Gore AH, Walekar LS, Anbhule PV, Patil SR, Kolekar GB. Turn-on fluorescence probe for selective and sensitive detection of D-penicillamine by CdS quantum dots in aqueous media: Application to pharmaceutical formulation. Sensors and Actuators B: Chemical. 2015;209:911-8.

10.   Convention TUSP. United States Pharmacopeia and National Formulary (USP 43-NF 38). Rockwell, MD.2020.

11.   Waseem A, Yaqoob M, Nabi A. Analytical applications of flow injection chemiluminescence for the determination of pharmaceuticals–A Review. Current Pharmaceutical Analysis. 2013;9:363-95.

12.   Song L, Guo Z. Sation and determination of chiral composition in penicillamine tablets by capillary electrophoresis in a broad pH range. Electrophoresis. 2012;33:2056-63.

13.   Trefi S. Assay of four psychotropic drugs chlorpromazine, clomipramine, amitriptyline and nortriptyline in tablets by a single HPLC method. International Journal of Pharmacy and Pharmaceutical Sciences. 2016;8(8):182-8.

14.   Zarembo JE, Warren RJ, Staiger DB. Quantitative determination of chlorpromazine. HCl in tablets, spansules, injectables, and bulk chemical by

nuclear magnetic resonance spectroscopy. J Assoc Off Anal Chem. 1978;61(1):52-4.

15. Plianwong S, Sripattanaporn A, Waewsa-nga K, Buacheen P, Opanasopit P, Ngawhirunpat T, et al. Operator care and eco-concerned development of a fast, facile and economical assay for basic nitrogenous drugs based on simplified ion-pair mini-scale extraction using safer solvent combined with drop-based spectrophotometry. Talanta. 2012;98:220-5.

16. Chanla J, Kanna M, Jakmunee J, Somnam S. Application of smartphone as a digital image colorimetric detector for batch and flow-based acid-base titration. Chiang Mai Journal of Science 2019;46(5):975 - 86.

17. Bandyopadhyay S, Rathod BB. The sound and feel of titrations: A smartphone aid for color-blind and visually impaired students. Journal of Chemical Education. 2017;94(7):946-9.

18. Rojanarata T, Sumran K, Nateetaweewat P, Winotapun W, Sukpisit S, Opanasopit P, et al. Microscale chemistry-based design of eco-friendly, reagent-saving and efficient pharmaceutical analysis: A miniaturized Volhard's titration for the assay of sodium chloride. Talanta. 2011;85(3):1324-9.

19. Rojanarata T, Waewsa-Nga K, Buacheen P, Opanasopit P, Ngawhirunpat T. Development of greener and safer assays for hydrochloride drugs: Photometric microtitration of phenylpropanolamine hydrochloride and metformin hydrochloride. Advanced Materials Research. 2012;361-363:1892-6.

20. Mok E, Retscher G, Wen C, editors. Initial test on the use of GPS and sensor data of modern smartphones for vehicle tracking in dense high rise environments. 2012 Ubiquitous Positioning, Indoor Navigation, and Location Based Service (UPINLBS); 2012 3-4 Oct. 2012.

21. Mehta S, Patel A, Mehta J. CCD or CMOS Image sensor for photography2015. 0291-4 p.

22. Sukariasih L, Erniwati, Sahara L, Hariroh L, Fayanto S. Studies the use of smartphone sensor for physics learning. International Journal of Scientific & Technology Research. 2019;8:862-70.

23. Sandstrom GM, Lathia N, Mascolo C, Rentfrow PJ. Putting mood in context: Using smartphones to examine how people feel in different locations. Journal of Research in Personality. 2017;69:96-101.

24. Merazzo KJ, Totoricaguena-Gorrino J, Fernandez-Martin E, Del Campo FJ, Baldrich E. Smartphone-enabled personalized diagnostics: Current status and future prospects. Diagnostics (Basel). 2021;11(6).

25. Saeb S, Zhang M, Karr CJ, Schueller SM, Corden ME, Kording KP, et al. Mobile phone sensor correlates of depressive symptom severity in daily-life behavior: An exploratory study. Journal of Medical Internet Research. 2015;17(7):e175.

26. Nam Y, Kong Y, Reyes B, Reljin N, Chon KH. Monitoring of heart and breathing rates using dual cameras on a smartphone. PLOS ONE. 2016;11(3):e0151013.

27. Thap T, Chung H, Jeong C, Hwang KE, Kim HR, Yoon KH, et al. High-resolution time-frequency spectrum-based lung function test from a smartphone microphone. Sensors (Basel). 2016;16(8).

28. Toy BC, Myung DJ, He L, Pan CK, Chang RT, Polkinhorne A, et al.

Smartphone-based dilated fundus photography and near visual acuity testing as inexpensive screening tools to detect referral warranted diabetic eye disease. Retina. 2016;36(5):1000-8.

29. Kim S, Cho D, Kim J, Kim M, Youn S, Jang JE, et al. Smartphone-based multispectral imaging: system development and potential for mobile skin diagnosis. Biomedical Optics Express. 2016;7(12):5294-307.

30. Abu-Ghanem S, Handzel O, Ness L, Ben-Artzi-Blima M, Fait-Ghelbendorf K, Himmelfarb M. Smartphone-based audiometric test for screening hearing loss in the elderly. Eur Arch Otorhinolaryngol. 2016;273(2):333-9.

31. Louw C, Swanepoel W, Eikelboom RH, Myburgh HC. Smartphone-Based Hearing Screening at Primary Health Care Clinics. Ear Hear. 2017;38(2):e93-e100.

32. Majumder S, Deen MJ. Smartphone Sensors for Health Monitoring and Diagnosis. Sensors (Basel). 2019;19(9).

33. Garcia IZ, Tome FEC, Belmonte UHH, Ramirez VA, Paredes JPR. Mobile digital colorimetry for the determination of ammonia in aquaculture applications. Computers and Electronics in Agriculture. 2021;181:105960.

34. Fahira AD, Saputro AH, editors. Colorimetric system based on android smartphone: Study case of total chlorine level prediction. 2021 8th International Conference on Electrical Engineering, Computer Science and Informatics (EECSI); 2021 20-21 Oct. 2021.

35. Peng B, Zhou J, Xu J, Fan M, Ma Y, Zhou M, et al. A smartphone-based colorimetry after dispersive liquid–liquid microextraction for rapid quantification of calcium in water and food samples. Microchemical Journal. 2019;149:104072.

36. Wongthanyakram J, Harfield A, Masawat P. A smart device-based digital image colorimetry for immediate and simultaneous determination of curcumin in turmeric. Computers and Electronics in Agriculture. 2019;166:104981.

37. Jarujamrus P, Meelapsom R, Pencharee S, Obma A, Amatatongchai M, Ditcharoen N, et al. Use of a smartphone as a colorimetric analyzer in paper-based devices for sensitive and selective determination of mercury in water samples. Analytical Sciences. 2018;34(1):75-81.

38. Shrivas K, Patel S, Sinha D, Thakur SS, Patle TK, Kant T, et al. Colorimetric and smartphone-integrated paper device for on-site determination of arsenic (III) using sucrose modified gold nanoparticles as a nanoprobe. Mikrochim Acta. 2020;187(3):173.

39. Nguyen H, Misbah I, Shih WC. Smartphone nano-colorimetry for on-demand multiplex lead and mercury detection and quantitation in drinking water. IEEE Sensors Journal. 2020;20(12):6685-91.

40. İncel A, Akın O, Çağır A, Yıldız ÜH, Demir MM. Smart phone assisted detection and quantification of cyanide in drinking water by paper based sensing platform. Sensors and Actuators B: Chemical. 2017;252:886-93.

41. Erdemir S, Malkondu S. On-site and low-cost detection of cyanide by simple colorimetric and fluorogenic sensors: Smartphone and test strip applications. Talanta. 2020;207:120278.

42. Santiago JB, Sevilla FB. Smartphone-based digital colorimetric measurement of dimethyl sulfide in wastewater. Microchemical Journal. 2022;172:106952.

43. Tsagkaris AS, Pulkrabova J, Hajslova J. Optical screening methods for pesticide residue detection in food matrices: Advances and emerging analytical trends. Foods. 2021;10(1).

44. Petryayeva E, Algar WR. Multiplexed homogeneous assays of proteolytic activity using a smartphone and quantum dots. Analytical Chemistry. 2014;86(6):3195-202.

45. Cheng N, Song Y, Fu Q, Du D, Luo Y, Wang Y, et al. Aptasensor based on fluorophore-quencher nano-pair and smartphone spectrum reader for on-site quantification of multi-pesticides. Biosensors and Bioelectronics. 2018;117:75-83.

46. Zhang D, Liu Q. Biosensors and bioelectronics on smartphone for portable biochemical detection. Biosensors and Bioelectronics. 2016;75:273-84.

47. Roda A, Michelini E, Cevenini L, Calabria D, Calabretta MM, Simoni P. Integrating biochemiluminescence detection on smartphones: Mobile chemistry platform for point-of-need analysis. Analytical Chemistry. 2014;86(15):7299-304.

48. McGonigle AJS, Wilkes TC, Pering TD, Willmott JR, Cook JM, Mims FM, et al. Smartphone Spectrometers. Sensors. 2018;18(1).

49. Koohkan R, Kaykhaii M, Sasani M, Paull B. Fabrication of a smartphone-based spectrophotometer and its application in monitoring concentrations of organic dyes. ACS Omega. 2020;5(48):31450-5.

50. Wilkes TC, McGonigle AJS, Willmott JR, Pering TD, Cook JM. Low-cost 3D printed 1 nm resolution smartphone sensor-based spectrometer: instrument design and application in ultraviolet spectroscopy. Optics Letters. 2017;42(21):4323-6.

51. Long KD, Yu H, Cunningham BT. Smartphone instrument for portable enzyme-linked immunosorbent assays. Biomedical Optics Express. 2014;5(11):3792-806.

52. Chang Y-C, Ge X, Wang L-J, Lee SS, Paulsen MH, Khan QM, et al. An ultra low-cost smartphone device for in-situ monitoring of acute organophosphorus poisoning for agricultural workers. Sensors and Actuators B: Chemical. 2018;275:300-5.

53. Keçili R, Ghorbani-Bidkorbeh F, Dolak İ, Canpolat G, Hussain CM. 2 - Smartphone-based optical and electrochemical sensing. In: Hussain C, editor. Smartphone-Based Detection Devices: Elsevier; 2021. p. 19-36.

54. Chaisiwamongkhol K, Labaidae S, Pon-in S, Pinsrithong S, Bunchuay T, Phonchai A. Smartphone-based colorimetric detection using gold nanoparticles of sibutramine in suspected food supplement products. Microchemical Journal. 2020;158:105273.

55. Su K, Qiu X, Fang J, Zou Q, Wang P. An improved efficient biochemical detection method to marine toxins with a smartphone-based portable system − Bionic e-Eye. Sensors and Actuators B: Chemical. 2016;238.

56. Oliveira GdC, Machado CCS, Inacio DK, Silveira Petruci JFD, Silva SG. RGB color sensor for colorimetric determinations: Evaluation and quantitative analysis of colored liquid samples. Talanta. 2022;241:123244.

57. Zhdanov A, Keefe J, Franco-Waite L, Konnaiyan KR, Pyayt A. Mobile phone based ELISA (MELISA). Biosensors and Bioelectronics. 2018;103:138-42.

58. Ruiz NL, Curto VF, Erenas MM, Lopez FB, Diamond D, Palma AJ, et al.

Smartphone-based simultaneous ph and nitrite colorimetric determination for paper microfluidic devices. Analytical Chemistry. 2014;86(19):9554-62.

59. Park H, Koh YG, Lee W. Smartphone-based colorimetric analysis of structural colors from pH-responsive photonic gel. Sensors and Actuators B: Chemical. 2021;345:130359.

60. Firdaus ML, Aprian A, Meileza N, Hitsmi M, Elvia R, Rahmidar L, et al. Smartphone coupled with a paper-based colorimetric device for sensitive and portable mercury ion sensing. Chemosensors. 2019;7(2).

61. Yu H, Le H, Lumetta S, Cunningham BT, Kaale E, Layloff T, editors. Smartphone-based thin layer chromatography for the discrimination of falsified medicines. 2016 IEEE SENSORS; 2016 30 Oct.-3 Nov. 2016.

62. Gad AG, Fayez YM, Kelani KM, Mahmoud AM. TLC-smartphone in antibiotics determination and low-quality pharmaceuticals detection. RSC Advances. 2021;11(31):19196-202.

63. Mulcare DC, Coward TJ. Suitability of a mobile phone colorimeter application for use as an objective aid when matching skin color during the fabrication of a maxillofacial prosthesis. Journal of Prosthodontics. 2019;28(8):934-43.

64. Vici A, Russo F, Lovisi N, Marchioni A, Casella A, Irrera F. Performance and Reliability Degradation of CMOS Image Sensors in Back-Side Illuminated Configuration. IEEE Journal of the Electron Devices Society. 2020;8:765-72.

65. Westland S. The CIE system. In: Chen J, Cranton W, Fihn M, editors. Handbook of Visual Display Technology. Berlin, Heidelberg: Springer Berlin Heidelberg; 2012. p. 139-46.

66. Shen L, Hagen JA, Papautsky I. Point-of-care colorimetric detection with a smartphone. Lab on a Chip. 2012;12(21):4240-3.

67. Rodman DC. Spectroscopy and RGB-colorimetry for quantification of plant pigment and fruit content in fruit drinks: LUND UNIVERSITY; 2018.

68. Hlaing WMM, Kruanetr S, Ruengsitagoon W. RGB colorimetric method for the quantitative analysis of levocetirizine tablets. Isan Journal of Pharmaceutical Sciences. 2020;16:65-75.

69. Caleb J, Alshana U, Ertaş N. Smartphone digital image colorimetry combined with solidification of floating organic drop-dispersive liquid-liquid microextraction for the determination of iodate in table salt. Food Chemistry. 2021;336:127708.

70. Guo J, Wong JXH, Cui C, Li X, Yu H-Z. A smartphone-readable barcode assay for the detection and quantitation of pesticide residues. Analyst. 2015;140(16):5518-25.

71. Phuangsaijai N, Jakmunee J, Kittiwachana S. Investigation into the predictive performance of colorimetric sensor strips using RGB, CMYK, HSV, and CIELAB coupled with various data preprocessing methods: a case study on an analysis of water quality parameters. Journal of Analytical Science and Technology. 2021;12(1):19.

72. Wang Y, Liu Y, Liu W, Tang W, Shen L, Li Z, et al. Quantification of combined color and shade changes in colorimetry and image analysis: water pH measurement as an example. Analytical Methods. 2018;10(25):3059-65.

73. Luka GS, Nowak E, Kawchuk J, Hoorfar M, Najjaran H. Portable device for the detection of colorimetric assays. Royal Society Open Science.

2017;4(11):171025.

74. Cantrell K, Erenas MM, de Orbe-Payá I, Capitán-Vallvey LF. Use of the hue parameter of the hue, saturation, value color space as a quantitative analytical parameter for bitonal optical sensors. Analytical Chemistry. 2010;82(2):531-42.

75. Coleman B, Coarsey C, Asghar W. Cell phone based colorimetric analysis for point-of-care settings. Analyst. 2019;144(6):1935-47.

76. Lamarca RS, Lima Gomes PCFd. A low cost method for carbamazepine, ciprofloxacin and norfloxacin determination in pharmaceutical formulations based on spot-test and smartphone images. Microchemical Journal. 2020;152:104297.

77. Li W, Zhang R, Wang H, Jiang W, Wang L, Li H, et al. Digital image colorimetry coupled with a multichannel membrane filtration-enrichment technique to detect low concentration dyes. Analytical Methods. 2016;8(14):2887-94.

78. Lima MJA, Nascimento CF, Rocha FRP. Feasible photometric measurements in liquid–liquid extraction by exploiting smartphone-based digital images. Analytical Methods. 2017;9(14):2220-5.

79. Costa RA, Morais CLM, Rosa TR, Filgueiras PR, Mendonça MS, Pereira IES, et al. Quantification of milk adulterants (starch, H2O2, and NaClO) using colorimetric assays coupled to smartphone image analysis. Microchemical Journal. 2020;156:104968.

80. Mane Y, Mashru R. New smartphone based colorimetric method development and validation of emtricitabine in bulk and tablet dosage form. Journal of Drug Delivery and Therapeutics. 2021;11(4):35-40.

81. Costa ABd, Helfer GA, Barbosa JLV, Teixeira ID, Santos RO, Santos RBd, et al. Photometrix uvc: A new smartphone-based device for digital image colorimetric analysis using pls regression. Journal of the Brazilian Chemical Society. 2021;32(3):675-83.

82. Hao A-Y, Wang X-Q, Mei Y-Z, Nie J-F, Yang Y-Q, Dai C-C. A smartphone-combined ratiometric fluorescence probe for specifically and visibly detecting cephalexin. Spectrochimica Acta Part A: Molecular and Biomolecular Spectroscopy. 2021;249:119310.

83. Xu J, Guo S, Jia L, Zhu T, Chen X, Zhao T. A smartphone-integrated method for visual detection of tetracycline. Chemical Engineering Journal. 2021;416:127741.

84. Wu YY, Liu BW, Huang P, Wu FY. A novel colorimetric aptasensor for detection of chloramphenicol based on lanthanum ion-assisted gold nanoparticle aggregation and smartphone imaging. Analytical and Bioanalytical Chemistry. 2019;411(28):7511-8.

85. Chitme HR. Smartphone applications for improved pharmaceutical care. International Journal of Pharmaceutical Sciences and Research. 2015;6:1000-7.

86. van de Pol JM, Geljon JG, Belitser SV, Frederix GWJ, Hövels AM, Bouvy ML. Pharmacy in transition: A work sampling study of community pharmacists using smartphone technology. Research in Social and Administrative Pharmacy. 2019;15(1):70-6.

87. Xu X, Rabina AS, Awad A, Rial C, Gaisford S, Basit AW, et al. Smartphone-enabled 3D printing of medicines. International Journal of Pharmaceutics.

2021;609:121199.

88. Riener CK, Kada G, Gruber HJ. Quick measurement of protein sulfhydryls with Ellman's reagent and with 4,4'-dithiodipyridine. Analytical and Bioanalytical Chemistry. 2002;373(4-5):266-76.

89. Akkaya H, Uysal G, Büke B, Gök G, Erel Ö, Karakükçü Ç. Evaluation of thiol/disulphide homeostasis as a novel predictor testing tool of early pregnancy viability. Taiwan J Obstet Gynecol. 2018;57(3):427-31.

90. Erel O, Neselioglu S. A novel and automated assay for thiol/disulphide homeostasis. Clinical Biochemistry. 2014;47(18):326-32.

91. Madgulkar AR, Bhalekar MR, Asgaonkar KD, Dikpati AA. Synthesis and characterization of a novel mucoadhesive derivative of xyloglucan. Carbohydrate Polymer. 2016;135:356-62.

92. Sahatsapan N, Rojanarata T, Ngawhirunpat T, Opanasopit P, Tonglairoum P. Synthesis of cysteine-functionalized chitosan as a mucoadhesive polymer for transmucosal drug delivery. Thai Journal of Pharmaceutical Sciences. 2018;42:176-9.

93. Samprasit W, Sarangkasiri K, Siriwutthirak J. Thiolated chitosan as mucoadhesive polymers for buccal drug delivery. Isan Journal of Pharmaceutical Sciences. 2018;12(4):1-13.

94. Kurz F, Hengst C, Kulozik U. RP-HPLC method for simultaneous quantification of free and total thiol groups in native and heat aggregated whey proteins. MethodsX. 2020;7:101112.

95. Chen X, Zhou Y, Peng X, Yoon J. Fluorescent and colorimetric probes for detection of thiols. Chemical Society Reviews. 2010;39(6):2120-35.

96. Robotham AC, Kelly JF. Detection and quantification of free sulfhydryls in monoclonal antibodies using maleimide labeling and mass spectrometry. MAbs. 2019;11(4):757-66.

97. Aronson JK. Meyler's side effects of drugs. sixteenth ed. Oxford, UK: Elsevier; 2016.

98. Hasnain MS, Nayak AK. Chapter 9 - Chitosan as mucoadhesive polymer in drug delivery. In: Hasnain MS, Beg S, Nayak AK, editors. Chitosan in Drug Delivery: Academic Press; 2022. p. 225-46.

99. M Ways TM, Lau WM, Khutoryanskiy VV. Chitosan and its derivatives for application in mucoadhesive drug delivery systems. Polymers (Basel). 2018;10(3):267.

100. Florea M, Ilie M. Ion-pair spectrophotometry in pharmaceutical and biomedical analysis: Challenges and perspectives. In: Sharmin E, Zafar F, editors. Spectroscopic Analyses. London: IntechOpen; 2017.

101. Prabhakar AH, Giridhar R. A rapid colorimetric method for the determination of Losartan potassium in bulk and in synthetic mixture for solid dosage form. Journal of Pharmaceutical and Biomedical Analysis. 2002;27(6):861-6.

102. El-Brashy A, Metwally M, El-Sepai F. Spectrophotometric determination of some fluoroquinolone antibacterials by ion-pair complex formation with cobalt (II) tetrathiocyanate. Journal of the Chinese Chemical Society. 2005;52.

103. Ashour S, Al-Khalil R. Simple extractive colorimetric determination of levofloxacin by acid-dye complexation methods in pharmaceutical preparations. Farmaco. 2005;60(9):771-5.

104. Mohamed GG. Spectrophotometric determination of ampicillin, dicluxacillin, flucloxacillin and amoxicillin antibiotic drugs: ion-pair formation with molybdenum and thiocyanate. Journal of pharmaceutical and biomedical analysis. 2001;24 4:561-7.

105. Prasad BB, Gupta S. Extraction-Spectrophotometric Determination of Certain-β-Lactam Antibiotics with Methylene Blue. Indian Journal of Pharmaceutical Sciences. 2000;62:261-6.

106. Rele R, Gurav PJ. A simple extractive spectrophotometricdetermination of loratadine, desloratadine and rupatadine from pharmaceutical formulations. International Journal of Pharma and Bio Sciences. 2012;3:P89-P95.

107. Salem Qarah NA, Basavaiah K, Swamy N. Ion-pair extractive spectrophotometric assay of terbinafine hydrochloride in pharmaceuticals and spiked urine using bromocresol purple. Journal of Applied Spectroscopy. 2016;83(4):694-702.

108. Kılıç V, Alankus G, Horzum N, Mutlu AY, Bayram A, Solmaz ME. Single-image-referenced colorimetric water quality detection using a smartphone. ACS Omega. 2018;3(5):5531-6.

109. Hong JI, Chang BY. Development of the smartphone-based colorimetry for multi-analyte sensing arrays. Lab Chip. 2014;14(10):1725-32.

110. Rani NU, Divya K, Sahithi G. New validated RP-HPLC method for simultaneous estimation of chlorpromazine and trihexyphenidyl HCl in tablets. International Journal of Advances in Pharmaceutical Analysis. 2014;4(4):134-7.

111. Mohamed GG, Frag EYZ, Zayed MA, Omar MM, Elashery SEA. Fabrication of chemically and in situ modified carbon paste electrodes for the potentiometric determination of chlorpromazine HCl in pure pharmaceutical preparations, urine and serum. New Journal of Chemistry. 2017;41(24):15612-24.

112. Jabbar H, Faizullah A. Flow injection analysis with chemiluminescence detection for determination of two phenothiazines. International Journal of Pharma Sciences and Research (IJPSR). 2015;6:474.

113. Tôrres AR, da Silva Lyra W, de Andrade SIE, Andrade RAN, da Silva EC, Araújo MCU, et al. A digital image-based method for determining of total acidity in red wines using acid–base titration without indicator. Talanta. 2011;84(3):601-6.

114. Somnam S, Kanna M. Flow-based titration with a colorimetric detection box using a smartphone for the determination of titratable acidity in coffee. ScienceAsia. 2020;46:52.

115. de Oliveira LMA, dos Santos VB, da Silva EKN, Lopes AS, Dantas-Filho HA. An environment-friendly spot test method with digital imaging for the micro-titration of citric fruits. Talanta. 2020;206:120219.

116. Nogueira SA, Sousa LR, Silva NKL, Rodrigues PHF, Coltro WKT. Monitoring acid–base titrations on wax printed paper microzones using a smartphone. Micromachines (Basel). 2017;8(5):139.

117. Karita S, Kaneta T. Acid–base titrations using microfluidic paper-based analytical devices. Analytical Chemistry. 2014;86(24):12108-14.

118. Myers NM, Kernisan EN, Lieberman M. Lab on Paper: Iodometric Titration on a Printed Card. Analytical Chemistry. 2015;87(7):3764-70.

119. Mbambo AT, Kruger HG, Mdluli PS, Madikizela LM. Fabrication and

application of a gold nanoparticle-based colorimetic device for the determination of NaCl in seawater and estuarine water. Journal of Nanoparticle Research. 2019;21(7):135.

120. Zhang C, Kim JP, Creer M, Yang J, Liu Z. A smartphone-based chloridometer for point-of-care diagnostics of cystic fibrosis. Biosens Bioelectron. 2017;97:164-8.

121. Ellman GL. Tissue sulfhydryl groups. Arch Biochem Biophys. 1959;82(1):70-7.

122. Choodum A, Kanatharana P, Wongniramaikul W, Nic Daeid N. Using the iPhone as a device for a rapid quantitative analysis of trinitrotoluene in soil. Talanta. 2013;115:143-9.

123. Moonrungsee N, Pencharee S, Jakmunee J. Colorimetric analyzer based on mobile phone camera for determination of available phosphorus in soil. Talanta. 2015;136:204-9.

124. Pohanka M. Photography by cameras integrated in smartphones as a tool for analytical chemistry represented by an butyrylcholinesterase activity assay. Sensors (Basel). 2015;15(6):13752-62.

125. Benedetti LPdS, dos Santos VB, Silva TA, Filho EB, Martins VL, Fatibello-Filho O. A digital image-based method employing a spot-test for quantification of ethanol in drinks. Analytical Methods. 2015;7(10):4138-44.

126. Moonrungsee N, Pencharee S, Jakmunee J. Colorimetric analyzer based on mobile phone camera for determination of available phosphorus in soil. Talanta. 2015;136:204-9.

127. Geng Z, Zhang X, Fan Z, Lv X, Su Y, Chen H. Recent progress in optical biosensors based on smartphone platforms. Sensors (Basel). 2017;17(11).

128. Acemel MA. Digitization of colorimetric measurements for quantitave analyses using a smartphone: OPEN UNIVERSITY OF CATALONIA; 2017.

129. Souza W, Oliveira M, Oliveira G, de Santana D, de Araujo R. Self-referencing method for relative color intensity analysis using mobile-phone. Optics and Photonics Journal. 2018;8:264-75.

130. Jia M-Y, Wu Q-S, Li H, Zhang Y, Guan Y-F, Feng L. The calibration of cellphone camera-based colorimetric sensor array and its application in the determination of glucose in urine. Biosensors and Bioelectronics. 2015;74:1029-37.

131. Schaefer S. Colorimetric water quality sensing with mobile smart phones [Text]2014.

132. Joshi DR, Adhikari N. An overview on common organic solvents and their toxicity. Journal of Pharmaceutical Research International. 2019.

133. Chemat F, Abert Vian M, Ravi HK, Khadhraoui B, Hilali S, Perino S, et al. Review of Alternative Solvents for Green Extraction of Food and Natural Products: Panorama, Principles, Applications and Prospects. Molecules. 2019;24(16).

134. Hossaini R, Chipperfield MP, Montzka SA, Leeson AA, Dhomse SS, Pyle JA. The increasing threat to stratospheric ozone from dichloromethane. Nature Communications. 2017;8(1):15962.

135. Fang X, Park S, Saito T, Tunnicliffe R, Ganesan AL, Rigby M, et al. Rapid increase in ozone-depleting chloroform emissions from China. Nature Geoscience. 2019;12(2):89-93.

136. Molinero AL, Cubero V, Irigoyen R, Piazuelo D. Feasibility of digital image colorimetry-Application for water calcium hardness determination. Talanta. 2013;103:236-44.

137. Porto ISA, Santos Neto JH, dos Santos LO, Gomes AA, Ferreira SLC. Determination of ascorbic acid in natural fruit juices using digital image colorimetry. Microchemical Journal. 2019;149:104031.

138. Lima MJA, Sasaki MK, Marinho OR, Freitas TA, Faria RC, Reis BF, et al. Spot test for fast determination of hydrogen peroxide as a milk adulterant by smartphone-based digital image colorimetry. Microchemical Journal. 2020;157:105042.

139. Worsfold PJ. SPECTROPHOTOMETRY | Overview. In: Worsfold P, Townshend A, Poole C, editors. Encyclopedia of Analytical Science (Second Edition). Oxford: Elsevier; 2005. p. 318-21.

140. Wang LJ, Naudé N, Demissie M, Crivaro A, Kamoun M, Wang P, et al. Analytical validation of an ultra low-cost mobile phone microplate reader for infectious disease testing. Clinica Chimica Acta. 2018;482:21-6.

141. Yetisen AK, Martinez-Hurtado JL, Garcia-Melendrez A, da Cruz Vasconcellos F, Lowe CR. A smartphone algorithm with inter-phone repeatability for the analysis of colorimetric tests. Sensors and Actuators B: Chemical. 2014;196:156-60.

142. Peng B, Chen G, Li K, Zhou M, Zhang J, Zhao S. Dispersive liquid-liquid microextraction coupled with digital image colorimetric analysis for detection of total iron in water and food samples. Food Chem. 2017;230:667-72.

143. Ballesteros J, Caleja-Ballesteros H, Villena M. Digital image-based method for iron detection using green tea (Camellia sinensis) extract as natural colorimetric reagent. Microchemical Journal. 2021;160:105652.

144. Thepchuay Y, Sonsa-ard T, Ratanawimarnwong N, Auparakkitanon S, Sitanurak J, Nacapricha D. Paper-based colorimetric biosensor of blood alcohol with in-situ headspace separation of ethanol from whole blood. Analytica Chimica Acta. 2020;1103:115-21.

145. Aydindogan E, Ceylan AE, Timur S. Paper-based colorimetric spot test utilizing smartphone sensing for detection of biomarkers. Talanta. 2020;208:120446.

VITA

NAME   Miss Noppharat Phadungcharoen

DATE OF BIRTH   17 August 1992

PLACE OF BIRTH   Bangkok

INSTITUTIONS   2017 – Present: Doctor of Philosophy, Pharmaceutical
ATTENDED   Sciences Ph.D. Program, Faculty of Pharmacy, Silpakorn
                     University, Thailand.
                     2011 – 2016:   Bachelor Degree, Doctor of
                     Pharmacy (1st Class Honors), Pharmaceutical Chemistry,
                     Faculty of Pharmacy, Silpakorn University, Thailand.

HOME ADDRESS   Ramkhamhaeng road, Minburi district, Bangkok 10510

PUBLICATION   Phadungcharoen, N., Patrojanasophon, P.,
                     Opanasopit, P., Ngawhirunpat, T., Chinsriwongkul, A. and
                     Rojanarata, T., 2019. Smartphone-based Ellman's
                     colourimetric methods for the analysis of d-penicillamine
                     formulation and thiolated polymer. International Journal of
                     Pharmaceutics, 558, p.120-127.

                         Phadungcharoen, N., Pengwanput, N., Nakapan, A.,
                     Sutitaphan, U., Thanomklom, P., Jongudomsombut, N.,
                     Chinsriwongkul, A. and Rojanarata, T., 2020. Ion pair
                     extraction coupled with digital image colorimetry as a
                     rapid and green platform for pharmaceutical analysis: An
                     example of chlorpromazine hydrochloride tablet assay.
                     Talanta, 219, p.121271.

                         Ruttanakorn K., Phadungcharoen N.,
                     Laiwattanapaisal W., Chinsriwongkul A.,Rojanarata T.,
                     2021. Smartphone-based technique for the determination
                     of a titration equivalence point from an RGB linear-
                     segment curve with an example application to miniaturized
                     titration of sodium chloride injections. Talanta, 23,
                     p.122602

AWARD RECEIVED   -